Microbiota impact *Drosophila* ageing via *Acetobacter, Tachykinin,* and *TkR99D*

Diana Marcu[1], David R Sannino[1], Anthony J Dornan[1,2], Rita Ibrahim[1], Atharv Kapoor[1], Miriam Wood[1], Adam J Dobson[1†]

1 - School of Molecular Biosciences, College of Medical Veterinary and Life Sciences, University of Glasgow, G12 8QQ, United Kingdom

2 - Cellular Analysis Facility - Shared Research Facilities, College of Medical Veterinary and Life Sciences, University of Glasgow, G12 8TA, United Kingdom

† For correspondence: adam.dobson@glasgow.ac.uk

Abstract

Gut microbiota exert an evolutionarily conserved influence on ageing, from invertebrates to humans. How do microbes that are physically confined to the gut lumen affect the systemic physiological process of ageing? In female *Drosophila*, we show that microbiota increase expression of the peptide hormone *Tachykinin (Tk)*, which corresponds to reduced lifespan. *Tk* is required for microbiota to shorten lifespan, with knockdown rendering flies constitutively long-lived even in the presence of an intact microbiota. This lifespan extension does not come with canonical costs to fecundity or feeding, but impacts on triacylglyceride (TAG) storage suggest adaptive functions in metabolic homeostasis. In flies with defined (gnotobiotic) microbiotas, we show that we can model *Tk*-dependent effects of microbiota on lifespan and TAG by monoassociation with *Acetobacter pomorum*. These effects require *Tk* in the midgut, and the cognate TK receptor *TkR99D* in neurons, implicating a microbiota-gut-neuron relay. This relay also appears to compromise gut barrier function in aged flies, indicating roles in healthspan as well as lifespan. However, the effect of *TkR99D* is independent of its reported role in insulin signalling and adipokinetic hormone signalling which, respectively, are canonical regulators of lifespan and TAG metabolism, suggesting a non-canonical role for *TkR99D* elsewhere in the nervous system. Altogether our results implicate a microbiota-gut-neuron axis in ageing, via a specific bacterium modulating activity of a specific and evolutionarily-conserved hormone.

Introduction

Gut microbiota influence lifespan and ageing across species. This effect appears to be evolutionarily conserved from the invertebrate models *Caenorhabditis elegans* and *Drosophila melanogaster* (Brummel et al., 2004; Cabreiro et al., 2013; Houthoofd et al., 2002; Matthews et al., 2020; Obata et al., 2018; Pryor et al., 2019; Sannino et al., 2018), through to vertebrates including fish and rodents (Gordon et al., 1966; Smith et al., 2017; Snyder et al., 1990; Tazume et al., 1991; Valenzano et al., 2015). Microbiota are also thought to play a role in human ageing (Johansen et al., 2023; OToole and Jeffery, 2015), supported by mendelian randomisation analysis indicating a putatively causal role (Liu et al., 2023) (but see also (Gagnon et al., 2023)). Gut microbiota are physically confined to the gut lumen, yet they influence ageing at an organismal level. By what mechanisms do microbiota modulate these systemic processes?

Evolutionary theories of ageing lead us to expect that mechanisms of ageing should have adaptive functions early in life, i.e. processes under positive selection in early life have deleterious pleiotropic effects in later life, which manifest as ageing (Williams, 1957) . Microbiota conform to this expectation, with their impacts on ageing appearing to trade off against widespread benefits to host health early in life. For example, microbiota commonly promote host development time, even with the same species of bacteria demonstrated to benefit host development across different phyla of animals (Schwarzer et al., 2016; Storelli et al., 2011; A. Wong et al., 2014). This motivates research to characterise how to decouple beneficial effects of microbiota early in life from deleterious effects in late life.

The capacity of microbiota to impact systemic processes, from a physically confined niche in the intestinal lumen, implicates endocrine signalling between organs. A role mediated by endocrine signalling is also consistent with the pleiotropic effects of microbiota, since hormones potently impact multiple traits. The relationship between microbiota and endocrine signalling may be bidirectional, with the microbiota altering how the gut - the biggest endocrine organ in animals - communicates lumen conditions to distal tissues, while distal tissues may direct how the gut manages the microbiota. Signalling in either direction has the potential to modulate ageing, with hormones serving as a key relay.

We chose to investigate these processes in the fruitfly *Drosophila melanogaster*. Flies can be reared axenic (i.e. without exogenous bacteria), and have a simple microbiota dominated by two families of bacteria (*Acetobacteraceae* and *Lactobacillaceae*). These bacteria can be cultured easily, and reintroduced to axenic fly eggs to generate gnotobiotic animals, enabling mapping of host phenotype to bacterial species. Fly genetics also enable tissue- and cell-type-specific genetic manipulations, e.g. expressing RNAi in specific locations, ideal for studying tissue-tissue signalling. We capitalised on these strengths to identify how defined bacteria modulate hormone signalling, and how ageing phenotypes are modulated by tissue-specific lesions in this signalling.

71 ## Results

72

73 **A role for *Tk* in lifespan regulation by microbiota**

74 First, we looked for evidence that microbiota modulate fly endocrine signalling. Hormone activity both
75 to and from the gut could be relevant to impact of microbiota; but since the gut is the site of physical
76 contact with gut microbiota, and also the largest endocrine organ, in which numbers of enteroendocrine
77 cells (EEs) can vary plastically in adults, we reasoned that EE counts could serve as a proxy for
78 microbial impacts of overall endocrine signalling capacity, even though other endocrine tissues could
79 also be affected. When we counted absolute numbers of EEs in whole guts (Figure 1A), we found more
80 cells in guts of conventionally-reared (CR) flies than in axenic flies, suggesting that microbiota enhance
81 capacity for endocrine signalling. Previous studies have shown that microbiota reduce the percentage
82 of EEs (Broderick et al., 2014; Liu et al., 2022), which we suggest may have been driven by an even
83 greater microbial promotion of other epithelial cell populations, reducing proportion of EEs despite
84 increased total numbers of EEs.

85

86 EEs express 14 peptide hormones (Hung et al., 2020) . We asked whether microbiota promote
87 expression of any of these specifically, by reanalysing public transcriptome data (Bost et al., 2018)
88 (Figure 1B). We were able to quantify expression of 13 genes, and we analysed the fourteenth (*Burs*)
89 by RT-qPCR (Figure S1). Four hormone genes were differentially expressed. Of these four, Tachykinin
90 (*Tk*) - which encodes orthologues of the mammalian neuropeptides Substance P and Neurokinins A/B
91 - appeared a particularly interesting candidate, because published data indicated that *Tk* knockdown
92 flies phenocopy the longer lifespan and metabolic phenotypes observed in axenic flies (Dobson et al.,
93 2015; Rewitz et al., 2024; Sannino et al., 2018; Song et al., 2014; A. C.-N. Wong et al., 2014). Since
94 the differential expression analysis was performed on public data, we validated the impact of microbes
95 on *Tk* expression in our lab stock (*Dahomey*) by RT-qPCR (Figure 1C). This correlation between
96 microbial promotion of *Tk* expression and shortening of lifespan, coupled to phenocopying between
97 axenic and *Tk* knockdown flies, led us to predict that *Tk* knockdowns would be constitutively long-lived
98 and their lifespan should no longer respond to microbiota.

99

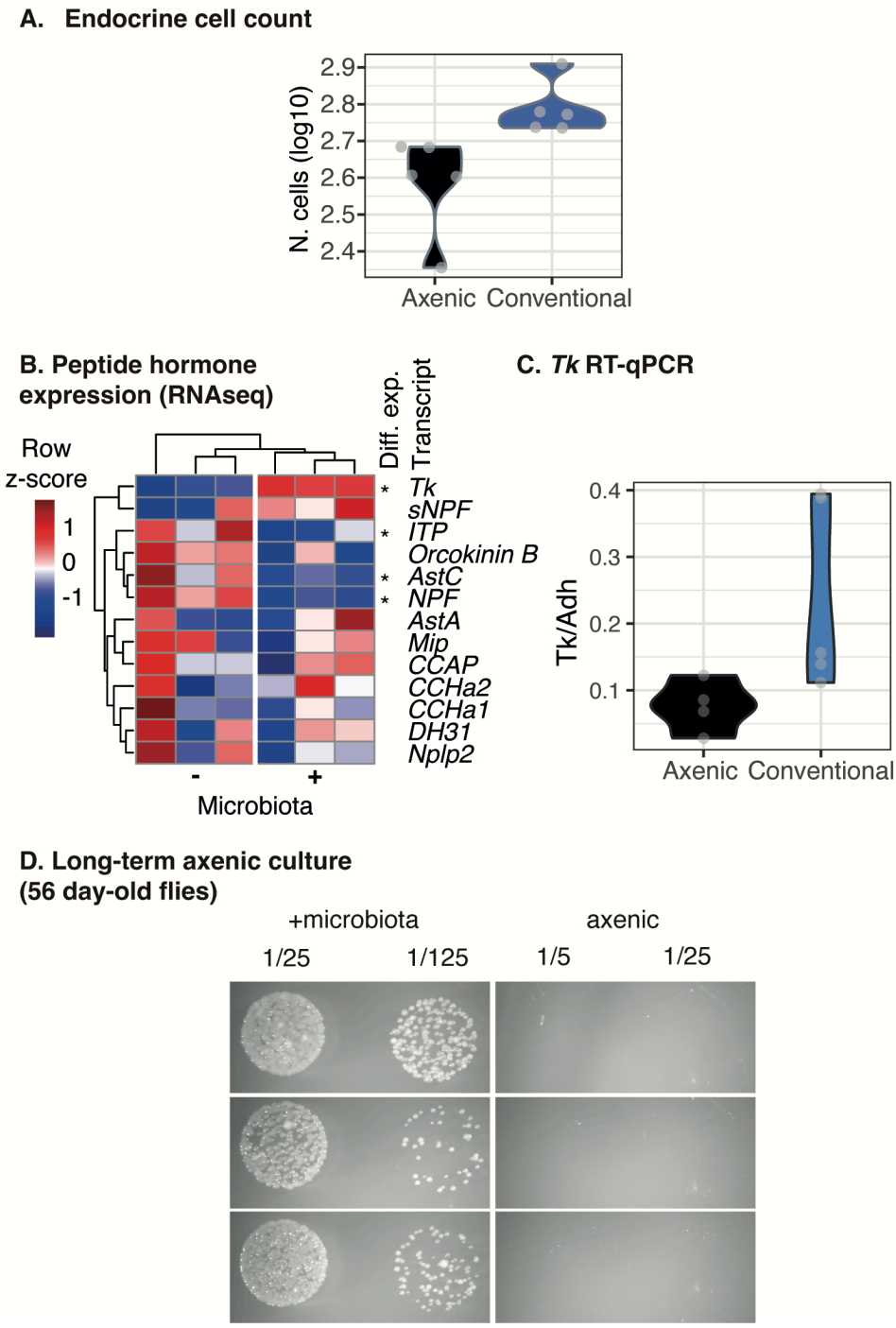

Figure 1. Basis for study: evidence that *Tk* responds to microbiota. A. Microbiota increase total number of enteroendocrine cells (EEs) in fly midgut. Number of GFP+ cells were scored in 5-day old *UAS-mCD8::GFP; Voila-Gal4* females. Wilcoxon test, W=25, P=0.008. **B.** Microbiota alter expression of peptide hormones in the *Drosophila* intestine. Transcriptome data from (Bost et al., 2018) were reanalysed. Expression of neuropeptide hormone gene transcripts are plotted, dendrograms show hierarchical clustering on Euclidian distance. Differentially expressed transcripts (DESeq2, FDR<0.1) are marked with an asterisk to right. Presence of microbiota increased expression of *Tachykinin* (top row). Software did not quantify *Burs* expression, so complementary RT-qPCR data were collected, showing no impact of microbiota (Figure S1). **C.** Confirmation that microbiota promote *Tk* expression.

110 Expression was quantified by RT-qPCR (using cDNA generated from midgut to complement RNA-seq
111 data). Wilcoxon test W=1, p=0.04. **D.** Confirmation of lifelong axenic culture without antibiotics.
112 Photographs show bacterial growth (or lack of) in homogenates of pools of 3 females, reared to day 56
113 of adulthood either with bacteria or axenic, serial dilutions indicated at top.
114
115 We tested our prediction by assessing impact of *Tk* knockdown in flies reared with/without a microbiota.
116 We reared flies under axenic conditions from embryo until death, to avoid potential off-target effects on
117 the fly of antibiotic feeding (Chatzispyrou et al., 2015; Moullan et al., 2015; Ronayne et al., 2023), after
118 confirming that we could maintain sterile culture conditions throughout the lifespan (Figure 1D). To
119 establish the genetic role of *Tk*, we first used a ubiquitous knockdown, to avoid in the first instance the
120 possibility that targeting one specific tissue may lead to compensatory expression in another. We drove
121 RNAi expression using an inducible ubiquitous driver (*Daughterless-GeneSwitch* a.k.a. *DaGS)*, which
122 we activated in 3-day-old adult females by feeding a chemical inducer, RU486 (henceforth, RU), thereby
123 avoiding any possible confounding impacts of knockdown during development. In all experiments, we
124 used female flies and a fully-factorial design.
125
126 Microbiota shortened lifespan relative to axenic controls (Figure 2A). However, Tk^{RNAi} blocked this
127 effect, rendering CR flies as long-lived as axenics. Cox Proportional Hazards analysis (CoxPH)
128 revealed a significant Tk^{RNAi}:microbiota interaction (p=0.05). To visualise specifically how the
129 experimental conditions differed from one another, we used estimated marginal means (EMMs) to
130 calculate *post hoc* differences between conditions, and to plot *post hoc* metrics of differences in survival
131 (multiplied by -1 such that higher values corresponded to extended lifespan). This analysis revealed a
132 significant shortening of lifespan by microbiota in CR flies relative to axenics, but Tk^{RNAi} blocked this
133 effect (Figure 2B), i.e. Tk^{RNAi} extended lifespan in conventional flies, but not in axenic flies. To confirm
134 the efficacy of *Tk* knockdown in conventional flies with an independent tool, we expressed a distinct
135 RNAi in conventional flies, which also extended lifespan (Figure S3); and an independent recent study
136 (Ahrentløv et al., 2025) also corroborates our findings. CR lifespan was not extended by RU in the
137 absence of the *UAS-*Tk^{RNAi} transgene (Figure S4), indicating that the *Tk*:microbiota interaction was
138 attributable to knockdown, not off-target effects of RU feeding; and bacterial load was not altered by
139 Tk^{RNAi} induction, suggesting that the lifespan difference is not due to altered density of microbiota
140 (Figure S5). Together, these results revealed that gut-microbial modulation of lifespan requires *Tk*.
141

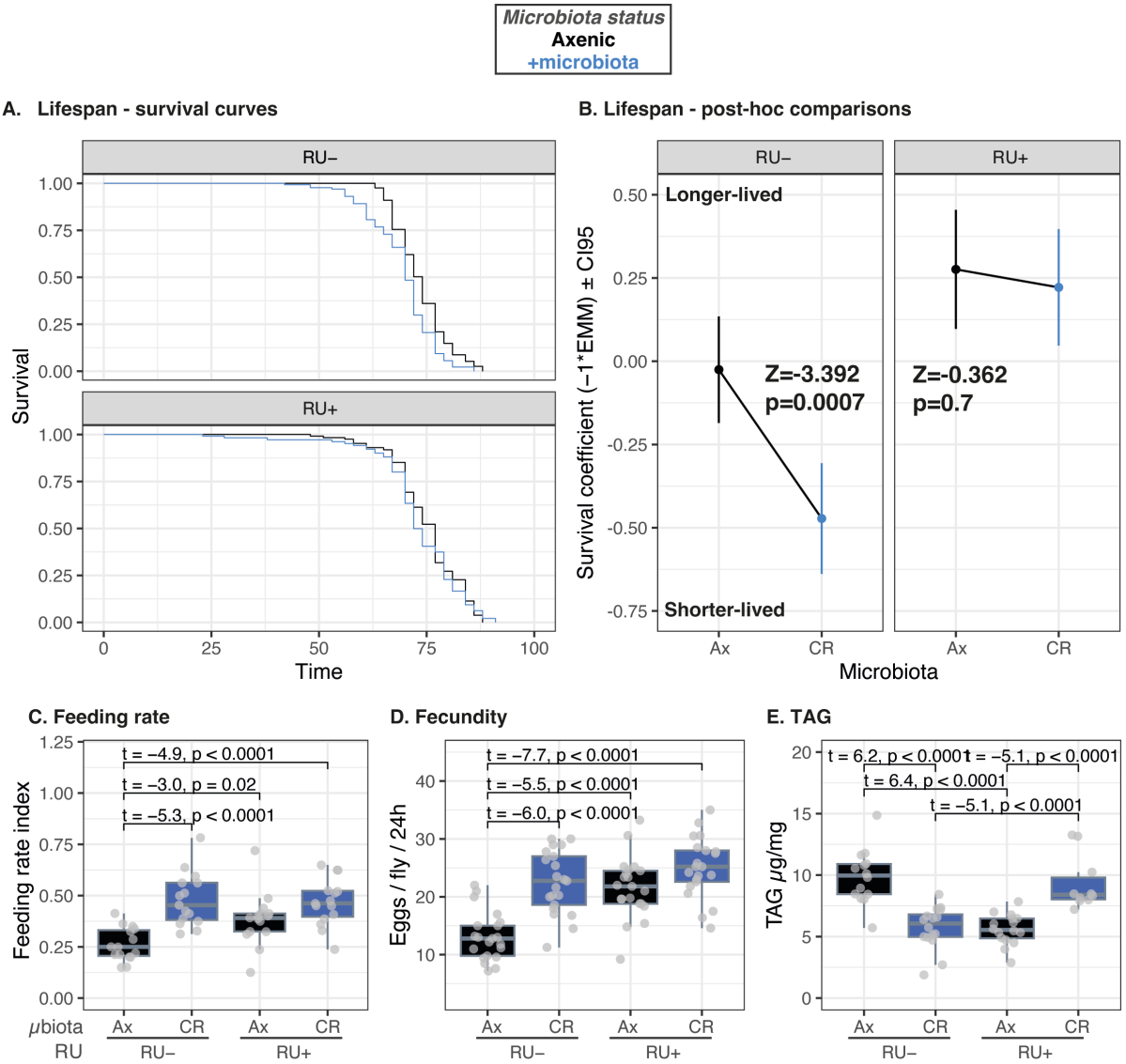

Figure 2. Ubiquitous *Tk* is required for microbiota to shorten lifespan and reduce TAG storage. **A.** Kaplan-Meier plots showing survival of axenic and conventionally-reared (CR) *DaGS;UAS-Tk^{RNAi}* flies, faceted by absence/presence (top/bottom) of transgene activation by RU486 (RU). Cox Proportional Hazards analysis revealed an RU:microbiota interaction (p=0.05). Axenic RU- n=135, axenic RU+ n=136, CR RU- n=135, CR RU+ n=135. **B.** Post-hoc analysis of survival data shown in A. Facets show estimated marginal means of Cox Proportional Hazards model (EMMs±95% confidence intervals (CI95)), multiplied -1*n to make higher values correspond to longer lifespan. Pairwise tests (text on facets) revealed impact of microbiota only in absence of RU. **C-D.** *Tk^{RNAi}* (RU+) does not block effect of microbiota on feeding rate (C) or fecundity (D). Feeding quantified as average proboscis extension rate per vial (n=5 mated females/vial, 10 days old after 7 days feeding on RU/vehicle.). Fecundity quantified as n. eggs laid per fly over 24h (n=5 females/vial). **E.** *Tk^{RNAi}* (RU+) blocks reduction of TAG by microbiota. Points give TAG μg mg^{-1} in pools of five flies. The result was replicated with an independent RNAi construct (Figure S3). Panels A-E generated with RNAi construct V330743. Panels

157 A-B, n=135-136 flies per condition. Panels C-E, Statistics on brackets are from *post-hoc* EMM analyses
158 of linear models (C, logit-transformed data), when significant differences were detected.
159
160 **Evidence for pleiotropic roles of *Tk* between lifespan and metabolism, but not canonical**
161 **tradeoffs with ageing**
162 Tachykinins are highly pleiotropic peptides (Nässel, 2025), and interventions that extend lifespan are
163 commonly associated with pleiotropic trade-offs early in life. For example, lifespan is expected to
164 anticorrelate reproduction in early life (Partridge et al., 2005), while feeding behaviour, naturally
165 selected to optimise growth and reproduction, is expected to be deleterious for ageing (Flatt, 2009;
166 Good and Tatar, 2001; Grandison et al., 2009; Mair et al., 2005). We therefore hypothesised that Tk^{RNAi}
167 might block beneficial effects of microbiota on reproduction or feeding in early life. We measured steady-
168 state feeding behaviour (proboscis extension) and a point measure of fecundity (egg laying over 24h),
169 after one week of Tk^{RNAi} induction in both axenic and CR flies. As expected, microbiota did indeed
170 increase feeding and egg laying in CR flies relative to axenics (Figure 2C-D), but Tk^{RNAi} did not reduce
171 either fecundity or feeding. Thus, longevity in CR Tk^{RNAi} flies appears not to be associated with canonical
172 costs.
173
174 We looked for alternative pleiotropic traits. Microbiota have evolutionarily-conserved effects on host
175 metabolism, with increased lipid storage observed in axenic hosts (Dobson et al., 2015; Turnbaugh et
176 al., 2006; Vijay-Kumar et al., 2010). Since *Tk* is also implicated in mobilising fly triglyceride (TAG) stores
177 (Song et al., 2014), we anticipated a potential tradeoff with lifespan. Without Tk^{RNAi}, microbiota reduced
178 TAG storage as expected, but Tk^{RNAi} blocked this effect in two replicate experiments with distinct Tk^{RNAi}
179 constructs (Figure 2E, Figure S6). These results suggested a pleiotropic role for *Tk* in managing
180 metabolic responses to microbiota in early life, with deleterious impacts for lifespan.
181
182 ***Acetobacter pomorum,* but not *Levilactobacillus brevis*, interacts with *Tk* to determine lifespan**
183 **and TAG**
184 Can the interaction between microbiota and *Tk* be attributed to particular gut bacteria? The fly
185 microbiota, while relatively simple, still contains numerous taxa, which vary among strains and
186 environments, but tend to contain families *Acetobacteraceae and Lactobacillaceae* (Brown et al., 2023;
187 Chandler et al., 2011; Staubach et al., 2012; Wang and Staubach, 2018; Wong et al., 2013). We
188 characterised the fly microbiota in our lab background by 16S rRNA amplicon sequencing, and identified
189 amplicon sequencing variants (ASVs). Most ASVs were assigned to the family *Acetobacteraceae*
190 (Figure 3a), and *Lactobacillaceae* were also present (among other families). *Acetobacter pomorum* and
191 *Levilactobacillus brevis* are two well-studied species that can be considered representatives of their
192 respective genera, on the basis of genome content (Newell et al., 2014) and phenotypic impacts (Newell
193 and Douglas, 2014). We asked whether either *A. pomorum* or *L. brevis* alone recapitulated impacts of
194 a CR microbiota on lifespan and TAG, and whether they interacted equivalently with Tk^{RNAi}.
195

196 We generated gnotobiotic flies, monoassociated with either *A. pomorum* (DmCS004) or *L. brevis*
197 (DmCS003), along with axenic controls, and tested whether lifespan impacts were blocked by
198 ubiquitous Tk^{RNAi} (Figure 3B-C). Without Tk^{RNAi}, axenic flies were longest-lived, and both bacteria
199 shortened lifespan. flies associated with *A. pomorum* (henceforth *Ap*-flies) were shortest-lived, and flies
200 associated with *L. brevis* (*Lb*-flies) were intermediate. However, Tk^{RNAi} induction rendered flies
201 constitutively long-lived, independent of microbiota association and equivalent to axenic controls. Thus,
202 Tk^{RNAi} blocked variation in lifespan caused by synthetic variation in the microbiota, and this effect was
203 strongest in *Ap*-flies.
204
205 We quantified *Tk* expression by RT-qPCR among axenic flies, *Lb*-flies and *Ap*-flies, and asked whether
206 change in expression upon knockdown (*DaGS, UAS-*Tk^{RNAi}) correlated lifespan outcome (Figure S7).
207 *Tk* expression was lowest in axenics, highest in *Ap*-flies, and intermediate in *Lb*-flies (Figure S7A), but
208 RU feeding arrested *Tk* expression across all three microbiota conditions - confirming universally
209 efficient knockdown - and this expression level was equivalent to control axenic flies (Figure S7A).
210 Plotting *Tk* expression against statistical coefficients (EMMs) of the corresponding survival data,
211 revealed a correlation across conditions between *Tk* expression values and lifespan (Figure S7B).
212 Thus, microbial modulation of lifespan appears to correspond to organismal expression of *Tk*.
213
214 We then asked whether specific bacteria and *Tk* interactively modulated TAG levels in youth (Figure
215 3E). We found reduced TAG in *Ap*-flies relative to axenic flies, and this effect was reversed by Tk^{RNAi},
216 consistent with the pleiotropic tradeoff we had observed in CR flies. However no interaction was
217 apparent between *L. brevis* and Tk^{RNAi}. Thus, *A. pomorum* was sufficient to modulate TAG in interaction
218 with *Tk*, but *L. brevis* was not. We also note that in both this experiment and the equivalents in CR flies
219 (Figure 2E, Figure S6), feeding RU to axenic flies reduced TAG. Since Tk^{RNAi} does not reduce *Tk*
220 expression in axenics (Figure S7), we interpret this as a possible off-target effect of RU, however such
221 an effect cannot account for the lack of difference between axenics without RU and *Ap*-flies/*Lb*-flies
222 with RU.
223
224 Altogether, these data demonstrated that *A. pomorum* is sufficient to fully recapitulate the impacts of a
225 complete microbiota on both lifespan and TAG, and interacts equivalently with ubiquitous Tk^{RNAi}. By
226 comparison the intermediate effects in *Lb*-flies argues against *Lactobacillaceae* playing a leading role
227 in the *Tk*-dependent regulation of lifespan and TAG.

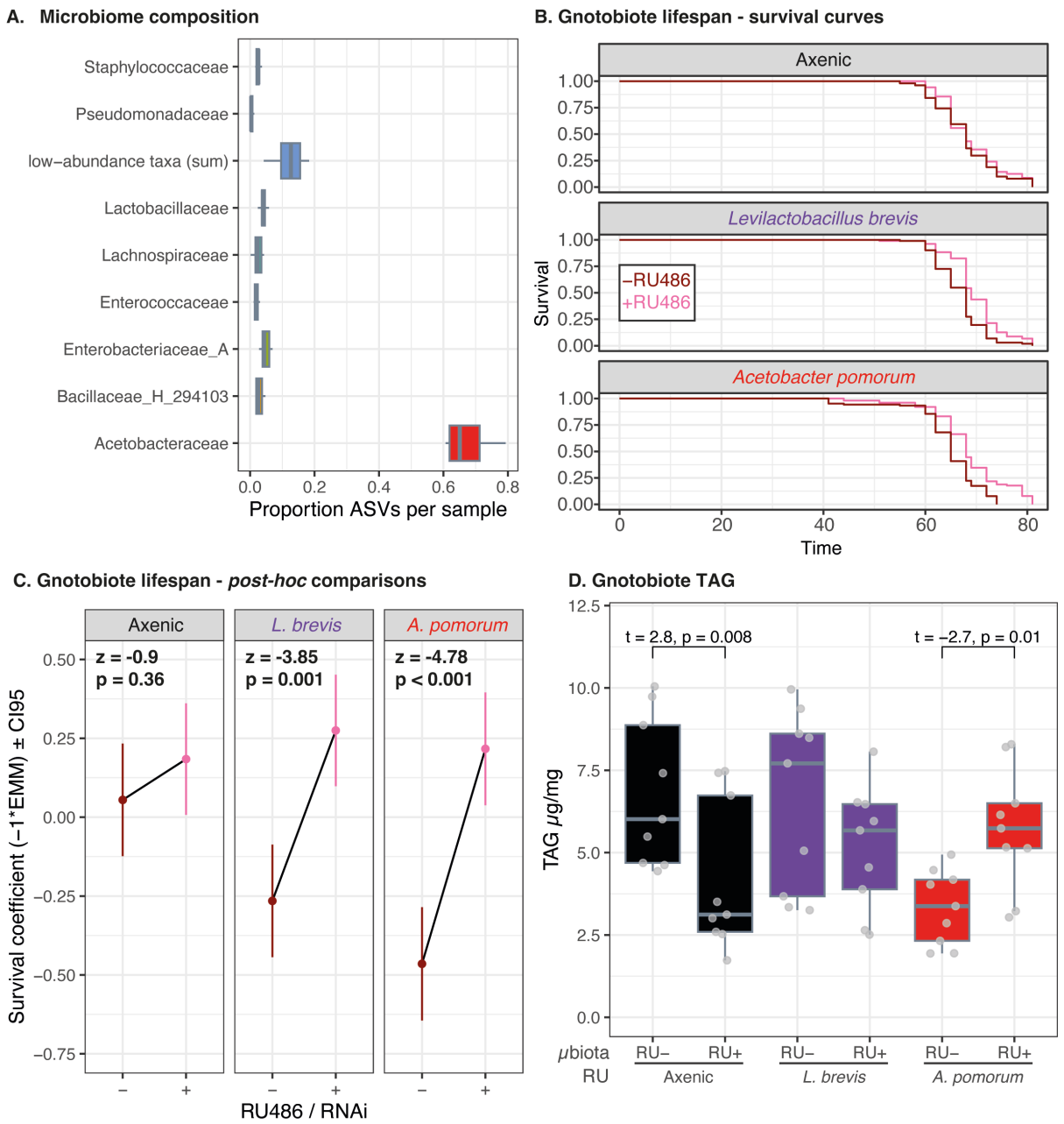

Figure 3. Phenotypic impact of a complete microbiota and interaction with ubiquitous *Tk*^{RNAi} is recapitulated fully by *Acetobacter pomorum*, but only partially by *Levilactobacillus brevis.* A. 16s rRNA amplicon sequencing reveals microbiota dominated by family *Acetobacteraceae* in the *Dahomey* fly background. Plot shows proportion ASVs per sample assigned to given families. "low abundance taxa" denotes a bin of all ASVs not assigned to one of the given families. ~170k reads per sample, n=10 samples. **B.** Kaplan-Meier plots showing survival of *DaGS;UAS-Tk*^{RNAi} flies (RNAi construct V330743), cultured either under axenic or gnotobiotic conditions. Gnotobiotic flies were cultured in monoassociation with either *Acetobacter pomorum* (*Ap*-flies) or *Levilactobacillus brevis* (*Lb*-flies). Plots are faceted by microbial condition. Cox Proportional Hazards analysis revealed an RU:microbiota interaction (p=0.02). Ap RU- n=105, Ap RU+ n=105, Ax RU- n=105, Ax RU+ n=104, Lb RU- n=105, Lb RU+ n=105. **C.** Post-hoc analysis of survival curves shown in B. Plots show a survival coefficient, calculated from estimated marginal means of Cox Proportional Hazards model (EMMs±95%

241 confidence intervals (CI95)), multiplied -1*n such that higher values correspond to longer lifespan.
242 Pairwise tests (text on facets) revealed effect of *Tk*^{RNAi} induction (+RU) was largest in *Ap*-flies,
243 intermediate in *Lb*-flies, and no effect was observed in axenics. **D.** *A. pomorum,* but not *L. brevis,*
244 recapitulates effects of a complete microbiota on TAG. Points give TAG μg mg^{-1} in pools of five flies
245 (n=9). Significant interaction of microbiota and *TkRNAi* (RU) was detected (ANOVA F=6.96, df=2,48,
246 p=0.002). Statistics on brackets are from *post-hoc* EMM analyses of linear models, when significant
247 differences were detected.
248
249 ***A. pomorum* modulates *Tk* expression in midgut but not CNS.**
250 Our initial experiments employed ubiquitous *Tk*^{RNAi}. From which specific tissue does *Tk* knockdown
251 mediate effects of the microbiota? Plotting steady-state *Tk* expression from the FlyAtlas2 database
252 (Leader et al., 2018) (i.e. from CR flies), revealed that *Tk* is enriched in neuronal and midgut tissues
253 (Figure 4A). We therefore characterised metrics of Tachykinin activity from these two tissues in axenic
254 flies, *Lb*-flies and *Ap*-flies. We examined *Tk* expression by RT-qPCR of RNA from heads and on
255 dissected midguts. *A. pomorum* increased *Tk* expression in midgut, but not in heads; while *L. brevis*
256 did not impact *Tk* expression in either tissue (Figure 4B). We used reporters to confirm intestinal
257 modulation of *Tk* expression. *Acetobacter* are thought to promote Tk signalling epigenetically, by
258 promoting histone lysine acetylation in *Tk+* cells (Jugder et al., 2021). We confirmed that lysine
259 acetylation was labile in *Tk+* EEs by feeding axenic flies with a histone deacetylase inhibitor,
260 trichostatin-A, and quantifying staining in *Tk+* cells in both anterior and posterior regions of the midgut
261 (Figure 4C-D). We then examined effects of microbiota, finding increased acetyl-lysine in *Tk+* cells of
262 *Ap*-flies, but not *Lb*-flies (Figure 4D). We asked whether this increase corresponded to elevated *Tk*
263 expression, and indeed *Tk* reporter expression (*Tk-T2A-Gal4>UAS*-GFP) was elevated in the anterior
264 midgut, but not posterior midgut (Figure 4E). Together, these results confirm previous observations that
265 *A. pomorum* increases lysine acetylation in *Tk+* EEs, suggesting possible epigenetic regulation or
266 priming of *Tk* regulation, but correspondence between lysine acetylation and *Tk* reporter expression
267 appears specific to certain regions of the midgut.
268
269 Having shown that *Tk* expression was activated specifically by *A. pomorum* in the midgut, but not by *L.*
270 *brevis*, we focussed specifically on *A. pomorum* in subsequent experiments.
271

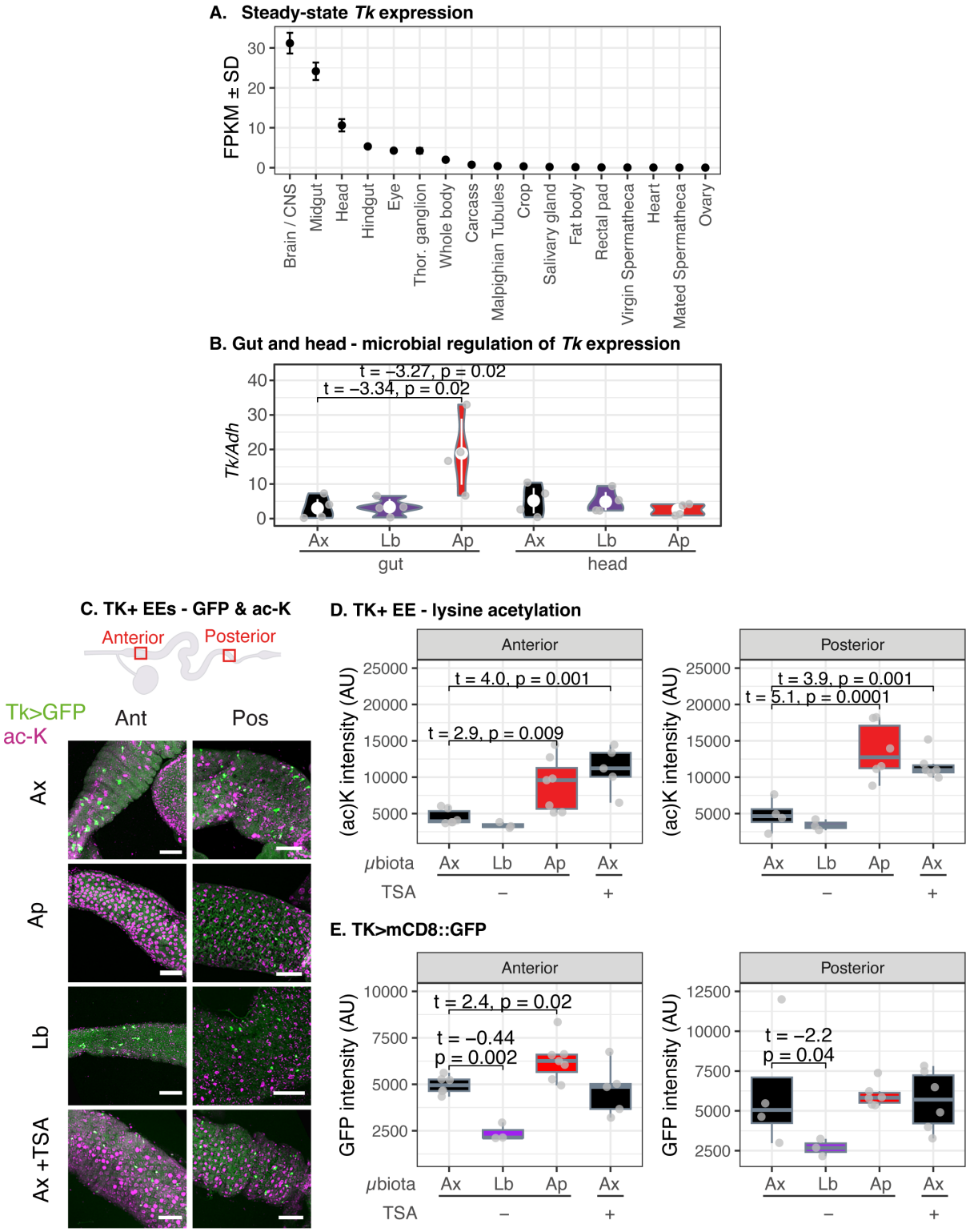

Figure 4. *A. pomorum* modulates intestinal *Tk* expression. A. *Tk* expression is enriched in nervous system and midgut tissues (data from FlyAtlas2). **B.** RT-qPCR of *Tk* in dissected midguts and heads of axenic and gnotobiotic flies indicates that expression is increased specifically in the midgut by *A. pomorum,* but not in the head; while *L. brevis* affects expression in neither tissue. White point and error bars show mean±SD. Statistics on brackets are from *post-hoc* EMM analyses of linear models, when significant differences were detected. **C.** Quantifying lysine acetylation and *Tk* promoter activity in *Tk*+ cells. Cartoon shows regions quantified in *Tk-Gal4/UAS-mCD8::GFP* flies with acetyl-lysine staining.

280 Scale bars=50μm. **D.** Lysine acetylation is increased specifically by *A. pomorum* in *Tk+* enteroendocrine
281 cells. Each point represents average fluorescence intensity for acetyl-lysine staining of ≥3 cells (marked
282 by *Tk>GFP*) per gut, in anterior and posterior regions. The HDAC inhibitor Trichostatin-A was fed to
283 axenic flies to confirm that increased histone acetylation is detectable by total acetyl-lysine staining.
284 Statistics from one-way ANOVA, showing comparisons relative to axenic control condition. **E.** *A.*
285 *pomorum* increases *Tk* promoter activity (*Tk-T2A-Gal4>UAS-GFP*) in anterior but not posterior midgut.
286 Each point represents average GFP intensity of ≥3 cells per gut, in anterior and posterior regions.
287 Statistics from one-way ANOVA, showing comparisons relative to axenic control condition.
288
289 **Intestine-directed *Tk* knockdown abrogates lifespan impact of *A. pomorum***
290 Next we asked whether *Tk* knockdown in the gut blocked the shortened lifespan of *Ap*-flies, using the
291 *Gal4-UAS* system. In the midgut, EEs are marked by *voila-Gal4*, but this construct is also expressed in
292 some neurons (Lin et al., 2022; Scopelliti et al., 2014) , posing a challenge for fully parsing effects of
293 neurons versus midgut EEs. We used a recently-developed intersectional strategy, in which *ChAT-*
294 *Gal80* represses neuronal *voila-Gal4* (Medina et al., 2024), directing Gal4 to the midgut while sparing
295 CNS. After confirming that this system was effective in our lab's genetic background (Figure S8), we
296 tested whether intestine-directed Tk^{RNAi} abrogated impact of *A. pomorum* on lifespan, including every
297 possible combination of *Voila-Gal4*, *ChAT-Gal80*, and *UAS-*Tk^{RNAi} in a fully-factorial design (Figure 5A-
298 B). Without Tk^{RNAi}, lifespan was reduced in *Ap*-flies relative to axenic controls. However, expressing
299 Tk^{RNAi} in all *voila+* cells (without *ChAT-Gal80*) blocked this effect of *A. pomorum* on lifespan. *ChAT-*
300 *Gal80* restored a small effect of microbiota, but the magnitude of effect (Z-score) was diminutive, only
301 ~27-40% of that observed in controls. A second CoxPH analysis of the same data confirmed an overall
302 4-way interaction of *A. pomorum* and the three transgenes, confirming that the impact of *A. pomorum*
303 was contingent on activation of Tk^{RNAi}, and the tissues in which it was activated (p=0.0005). These
304 analyses indicated that *Tk* in *Voila+* cells was obligately required for *A. pomorum* to modulate lifespan,
305 and that the majority of this effect was explained by the intestine.
306
307 For further validation we conducted a second lifespan experiment, using independent genetic tools
308 (Rewitz et al., 2024) to direct Tk^{RNAi} specifically to *Tk*+ EEs, with *Gal4* expressed from the *Tk* locus (*Tk-*
309 *T2A-Gal4*), recombined with a transgene expressing *Gal80* under control of a fragment of *nSyb*
310 promoter (*R57C10-Gal80*), which is expected to lead to pan-neuronal *Gal80* expression as another
311 means to attenuate neuronal Gal4 activity (Kubrak et al., 2022; Malita et al., 2022; Rewitz et al., 2024).
312 We again detected an *A. pomorum*-by-genotype effect (Figure 5C-D), with the lifespan-shortening effect
313 of *A. pomorum* attenuated by *Tk* knockdown, and post-hoc tests showing only a marginal effect of *A.*
314 *pomorum* on lifespan upon Tk^{RNAi} induction (p=0.08). Independent *Gal4* and *Gal80* transgenes
315 therefore corroborated the finding that intestinal *Tk* is required for the majority of *A. pomorum*'s lifespan-
316 shortening effect.

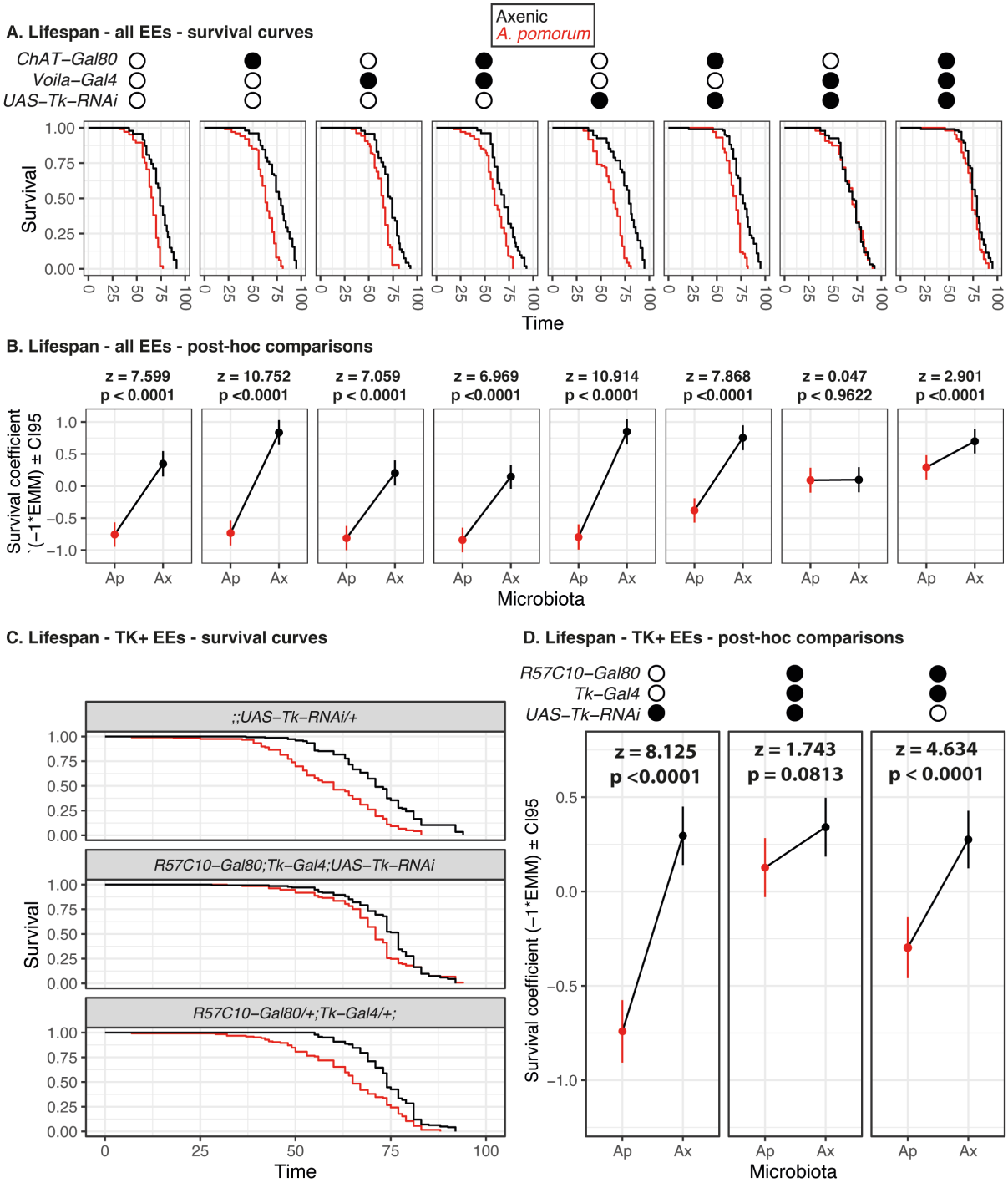

Figure 5. Gut-directed *Tk*^{RNAi} abrogates lifespan shortening by *A. pomorum*. A. Kaplan-Meier survival plots of the indicated genotypes in presence/absence of *A. pomorum*, with knockdown activated by *Voila-Gal4,* in presence/absence of *ChAT-Gal80*. Statistics from *post-hoc* tests of CoxPH model. Genotypes indicated above panels. See Figure S8 for tissue-specificity of transgene combinations. All conditions n=105. **B.** *Post-hoc* analysis of survival model reveals attenuated lifespan response to *A. pomorum* with midgut-directed *Tk*^{RNAi} (Genotypes as in A). Text indicates differences between *A. pomorum* and axenic flies in the given genotype. CoxPH analyses detected significant interactions both for microbiota*genotype (p<2.2e-16) and for Microbiota*:Voila-Gal4:ChAT-Gal80:UAS-TkRNAi* (p=0.0005). **C.** Kaplan-Meier survival plots of the indicated genotypes in presence/absence of *A.*

327 *pomorum*, with knockdown activated by *Tk-T2A-Gal4,* and neuronal activity suppressed by *R57C10-*
328 *Gal80*. **D.** *Post-hoc* analysis of survival model reveals attenuated lifespan response to *A. pomorum*
329 with Tk^{RNAi} directed to midgut by *Tk-T2A -Gal4* and *R57C10-Gal80*. Statistics from *post-hoc* tests of
330 CoxPH model, indicating differences between *Ap*-flies and axenic flies in the given genotype. CoxPH
331 detected overall genotype-by- *A. pomorum* interaction (p=2.46e-5).
332
333
334 **Role for neuronal $TkR99D^{RNAi}$ in host ageing effects of *A. pomorum***
335 We asked which receptors might mediate the *Tk*-dependent response to *A. pomorum*, and from which
336 tissues. The fly genome expresses two cognate Tk receptors (TkRs) - *TkR86C* and *TkR99D* - which
337 have different affinities for the six peptides encoded by *Tk* (Nässel et al., 2019), and distinct
338 physiological roles. Plotting steady-state *TkR86C* and *TkR99D* expression, again using FlyAtlas2 (CR
339 fly) data (Leader et al., 2018), revealed that both TkRs were most strongly expressed in CNS (Figure
340 6A). We expected that knocking down either one or both TkRs should extend lifespan in *Ap*-flies,
341 mimicking effects of *Tk* knockdown.
342
343 We tested the lifespan impacts of adult-onset TkR manipulation. RNAi constructs were developmentally
344 lethal when crossed to ubiquitous drivers (*DaGS* and *ActGS*), even in the absence of inducer (RU), so
345 instead we established lifespan experiments using the pan-neuronal driver, *Elav-GS*. Lifespan was
346 shorter in *Ap*-flies relative to controls, and RNAi against each TkR interacted with the lifespan effect of
347 *A. pomorum*, but in notably distinct ways. $TkR86C^{RNAi}$ had no effect in *Ap*-flies, but axenics were no
348 longer long-lived (Figure 6B-C): this reveals an interaction with *A. pomorum* but does not recapitulate
349 that of Tk^{RNAi}, suggesting that TkR86C likely does not signal downstream of the *A. pomorum-Tk* relay.
350 By contrast, $TkR99D^{RNAi}$ extended lifespan in *Ap*-flies, equivalent to axenics (Figure 6D-E). The most
351 parsimonious explanation of these results is an *Acetobacter*-Tk-TkR99D relay, which shortens lifespan.
352
353 In fly midgut, TkR99D reportedly plays a role in mobilising lipid stores in enterocytes of the fly midgut
354 (Song et al., 2014), prompting us to ask whether it may play an additional role in lifespan from these
355 cells. However, expressing $TkR99D^{RNAi}$ with the enterocyte driver *Mex-GS* did not extend *Ap*-flies
356 lifespan, suggesting that the *A. pomorum*-Tk relay signals gut-nonautonomously (Figure S9).
357
358 Finally, we asked whether lifespan extension in axenics and upon knockdown of *TkR99D* was
359 accompanied by improved health in older flies (i.e. healthspan). Fly microbiota compromise healthspan
360 by promoting gut barrier dysfunction in aged animals, characterised by permeability which shortly
361 precedes death (Clark et al., 2015; Regan et al., 2016; Rera et al., 2012; Zane et al., 2023) . We
362 therefore tested whether *A. pomorum* promoted gut barrier dysfunction, and whether this could be
363 rescued by $TkR99D^{RNAi}$ induction. We aged axenic and *Ap*-flies, with $TkR99D^{RNAi}$ from day 3 of
364 adulthood onwards, before feeding on a blue dye to report gut permeability after 56 days (Figure 6F).
365 *Ap*-flies indeed exhibited a higher rate of gut permeability than axenics, but $TkR99D^{RNAi}$ rescued the

366 pathology to a level that was not significantly different from axenics. Thus, *TkR99D*^{RNAi} can ameliorate
367 deleterious impacts of *A. pomorum* on late-life health, suggesting that the putative *A. pomorum-Tk-*
368 *TkR99D* relay limits late-life health.
369

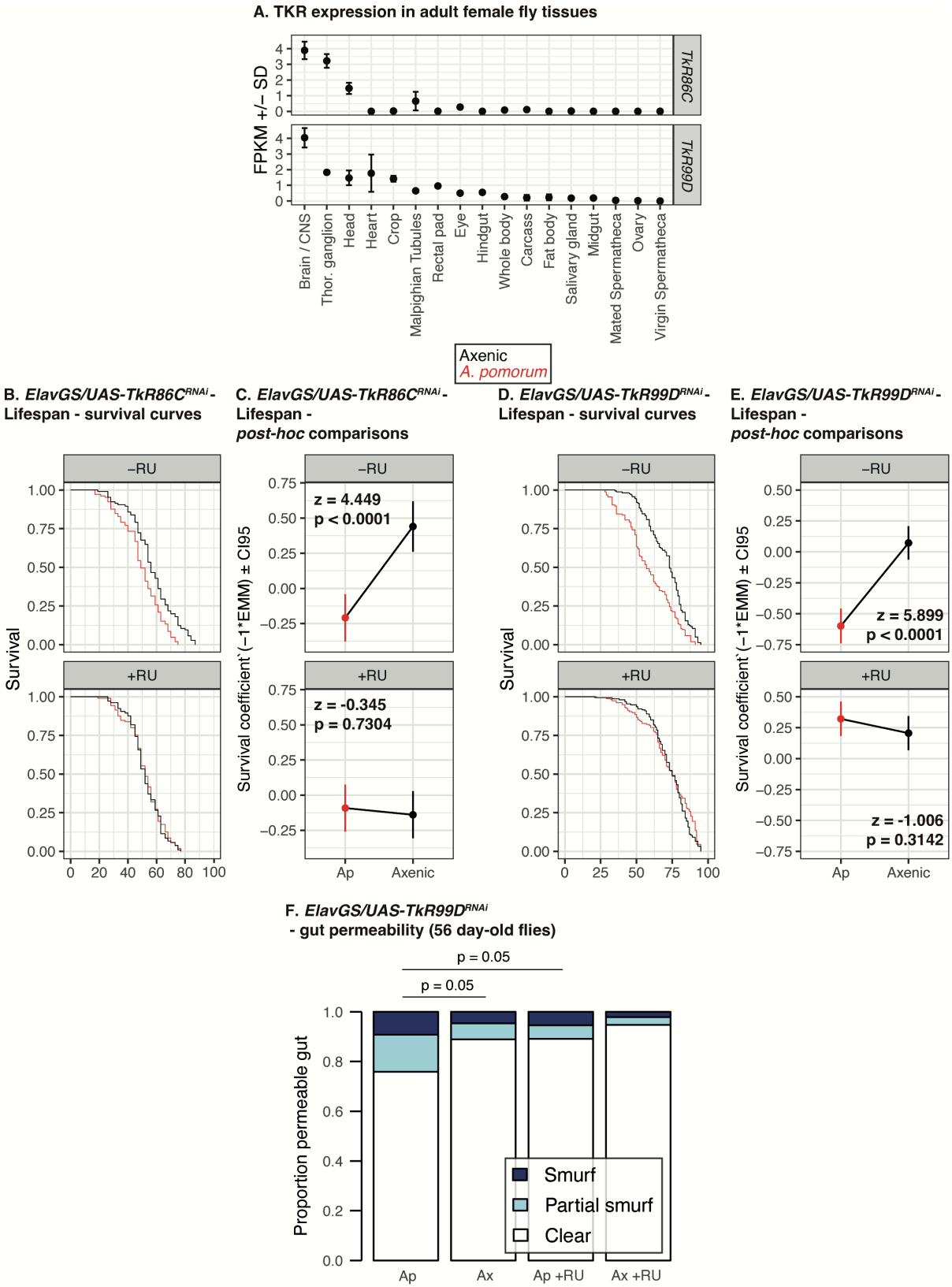

370

371 **Figure 6. Pan-neuronal *TkR99D^{RNAi}* abrogates lifespan impact of *A. pomorum*. A.** FlyAtlas data
372 showing expression of the two cognate *Drosophila* Tk receptors, *TkR86C* and *TkR99D*, among adult
373 female tissues. **B.** Kaplan-Meier survival plots of *Elav-GS; UAS-TkR86C^{RNAi}* flies in presence/absence
374 of *A. pomorum*, with knockdown activated by RU486 feeding (bottom facet). CoxPH detected significant
375 microbiota*RU interaction (p=0.0005). All conditions n=105. **C.** Post-hoc analysis of data from B
376 showing that *TkR86C^{RNAi}* induction locks axenic flies into a shortened lifespan. Text indicates
377 differences between *A. pomorum* and axenic flies in each given RU condition. **D.** Kaplan-Meier survival
378 plots of *Elav-GeneSwitch; UAS-TkR99D^{RNAi}* flies in presence/absence of *A. pomorum*, with knockdown
379 activated by RU486 feeding (bottom facet). CoxPH detected significant microbiota*RU interaction
380 (p=1.362e-6). Ap RU- n=163, Ap RU+ n=161, Axenic RU- n=165, Axenic RU+ n=164 (pool of two
381 replicate experiments). **E.** Post-hoc analysis of data from B showing that *TkR99D^{RNAi}* induction blocks
382 shortening of lifespan by *A. pomorum*. Text indicates differences between *A. pomorum* and axenic flies
383 in each given RU condition. **F.** Neuronal *TkR99D^{RNAi}* blocks onset of gut permeability ("smurf"
384 phenotype) in aged flies. Bars show relative frequencies of flies with blue dye appearing to permeate
385 through all tissues ("full smurf") and through abdomen/thorax ("partial smurf"). χ^2=16.126, DF=6,
386 p=0.013. P-values on figure from chi-square tests of each given pair of columns, shown when
387 differences were observed (otherwise omitted).
388
389 **Lifespan and metabolic impacts of *A. pomorum* are not explained by *TkR99D* in insulin-**
390 **producing cells**
391 What happens downstream of the putative *A. pomorum*-Tk-TkR99D relay? Reduced insulin signalling
392 promotes healthy ageing across species, with lifespan and other benefits reported in flies, nematodes
393 and rodents, and genetic associations indicating potential conservation in humans (Clancy et al., 2001;
394 Kenyon et al., 1993; Selman et al., 2008; Slagboom et al., 2017) . *A. pomorum* is reported to activate
395 insulin signalling (S. Shin et al., 2011), while *TkR99D* expression is reported in insulin-producing cells
396 (IPCs) in the fly brain (Birse et al., 2011), ablation of which extends lifespan (Alic et al., 2014; Broughton
397 et al., 2005). We therefore hypothesised that Tk-TkR99D signalling impacts ageing by serving as a
398 relay between the gut microbiota and IPCs (Figure 7A).
399
400 We tested whether insulin signalling was required for lifespan to respond to *A. pomorum*. The forkhead
401 box-O transcription factor dFOXO, encoded by the *dFoxO* locus, is obligately required for longevity
402 upon reduced insulin signalling (Slack et al., 2015, 2011). dFOXO is retained in cytoplasm of Ap-flies,
403 consistent with activated insulin signalling (S. Shin et al., 2011). We recombined a dFOXO null mutation
404 (*dFoxO$^{\Delta 94}$*) with transgenes to knock down *Tk* ubiquitously, performed lifespan assays, and used Cox
405 proportional hazards analysis to test for an *A. pomorum*Tk*dFoxO* interaction (Figure 7B-C). We
406 observed a significant three-way interaction (CoxPH p=5.384e-05) – indicating that *dFoxO$^{\Delta 94}$*
407 modulated the microbiota-*Tk* interaction – and then used post-hoc tests to dissect the co-dependence
408 of the three experimental variables (Table 1). In controls without *Tk* knockdown, *A. pomorum* shortened
409 lifespan relative to axenics in wild-type flies, but *dFoxO$^{\Delta 94}$* flies exhibited a diminished but still-significant

410 shortening of lifespan by *A. pomorum*. Without *dFoxO*$^{\Delta 94}$*, Tk* knockdown blocked lifespan response by
411 rendering *Ap*-flies long-lived. In the *dFoxO*$^{\Delta 94}$ background*, Tk* knockdown did not extend lifespan, in
412 either *Ap*-flies or axenics. However, unexpectedly, *Tk*^{RNAi} ceased to block the effect of *A. pomorum* in
413 the *dFoxO*$^{\Delta 94}$ background. Thus, in summary, (A) *dFoxO* is partially required for lifespan effect of *A.*
414 *pomorum*, (B) *dFoxO* is required for lifespan extension upon *Tk* knockdown, and (C) *dFoxO* is required
415 for *A. pomorum* and *Tk* knockdown to have an interactive effect on lifespan. We interpret that *dFoxO*
416 potentiates the putative *A. pomorum*-Tk-TkR99D relay.

417

Table 1. *dFoxO* is partially required for microbiotaTk* interaction for lifespan: post-hoc pairwise comparisons (EMMeans)**

contrast	estimate	SE	z.ratio	p.value
(Ax WT RU-) - (Ap WT RU-)	-1.12	0.13	-8.76	6.38E-14
(Ax WT RU-) - (Ax dFoxOΔ RU-)	-0.92	0.12	-7.51	1.75E-12
(Ax WT RU-) - (Ap dFoxOΔ RU-)	-1.51	0.13	-11.87	0
(Ax WT RU-) - (Ax WT RU+)	-0.02	0.12	-0.15	0.9999999
(Ax WT RU-) - (Ap WT RU+)	-0.21	0.12	-1.77	0.63954118
(Ax WT RU-) - (Ax dFoxOΔ RU+)	-0.85	0.13	-6.79	3.21E-10
(Ax WT RU-) - (Ap dFoxOΔ RU+)	-1.48	0.13	-11.65	0
(Ap WT RU-) - (Ax dFoxOΔ RU-)	0.2	0.12	1.66	0.71153814
(Ap WT RU-) - (Ap dFoxOΔ RU-)	-0.39	0.12	-3.16	0.03369588
(Ap WT RU-) - (Ax WT RU+)	1.1	0.13	8.6	7.16E-14
(Ap WT RU-) - (Ap WT RU+)	0.91	0.13	7.27	1.00E-11
(Ap WT RU-) - (Ax dFoxOΔ RU+)	0.27	0.13	2.13	0.39332695
(Ap WT RU-) - (Ap dFoxOΔ RU+)	-0.36	0.12	-2.96	0.06098085
(Ax dFoxOΔ RU-) - (Ap dFoxOΔ RU-)	-0.59	0.12	-4.99	1.70E-05
(Ax dFoxOΔ RU-) - (Ax WT RU+)	0.9	0.12	7.34	5.87E-12
(Ax dFoxOΔ RU-) - (Ap WT RU+)	0.71	0.12	5.93	8.56E-08
(Ax dFoxOΔ RU-) - (Ax dFoxOΔ RU+)	0.06	0.12	0.54	0.99943704
(Ax dFoxOΔ RU-) - (Ap dFoxOΔ RU+)	-0.57	0.12	-4.77	5.07E-05
(Ap dFoxOΔ RU-) - (Ax WT RU+)	1.49	0.13	11.7	0
(Ap dFoxOΔ RU-) - (Ap WT RU+)	1.3	0.12	10.45	7.78E-14
(Ap dFoxOΔ RU-) - (Ax dFoxOΔ RU+)	0.65	0.12	5.35	2.43E-06
(Ap dFoxOΔ RU-) - (Ap dFoxOΔ RU+)	0.02	0.12	0.19	0.99999961
(Ax WT RU+) - (Ap WT RU+)	-0.19	0.12	-1.61	0.74370666
(Ax WT RU+) - (Ax dFoxOΔ RU+)	-0.84	0.13	-6.63	9.28E-10
(Ax WT RU+) - (Ap dFoxOΔ RU+)	-1.47	0.13	-11.49	0
(Ap WT RU+) - (Ax dFoxOΔ RU+)	-0.64	0.12	-5.23	4.63E-06
(Ap WT RU+) - (Ap dFoxOΔ RU+)	-1.27	0.12	-10.23	6.75E-14
(Ax dFoxOΔ RU+) - (Ap dFoxOΔ RU+)	-0.63	0.12	-5.14	7.52E-06

418

419

420

421 To assess directly the role of tissues reported to express *TkR99D* (Birse et al., 2011), we turned to the
422 IPCs. We first tested whether ablating these cells by expressing the pro-apoptotic factor *Rpr* would
423 block lifespan response to *A. pomorum*, reasoning that a role for these cells in response to the bacteria
424 would be shown by a lack of response following ablation. Lifespan was again shortened in *Ap*-flies
425 relative to axenic controls. However this effect was blocked by adult-onset *Rpr* expression in IPCs
426 (using the *Dilp2-GS* driver) (Figure 7D-E), and we detected an overall microbiota*RU interaction
427 (CoxPH p=0.003). This indicated a role for IPCs in lifespan shortening by *A. pomorum*. To test whether
428 TkR99D activation could account for this effect we expressed $TkR99D^{RNAi}$ in IPCs, and assayed
429 expression of the three insulin-like peptides expressed therein (*Ilp2, Ilp3, Ilp5*) by RT-qPCR of heads
430 (Figure 7F, Table 2). *Ilp2* exhibited no response to *A. pomorum* or $TkR99D^{RNAi}$.(linear model,
431 microbiota:RU interaction $F_{1,24}$=0.424, p=0.5) However, for *Ilp3* and *Ilp5*, *A. pomorum* promoted
432 expression, and this effect was blocked by $TkR99D^{RNAi}$ induction (linear models, microbiota:RU
433 interactions *Ilp3* $F_{1,24}$=23.404, p=0.0001, *Ilp5* $F_{1,24}$=29.261, p<0.0001.) Specifically, *Ilp3* and *Ilp5*
434 expression levels were increased in *Ap*-flies, but these effects were absent upon $TkR99D^{RNAi}$ induction
435 (Table 2).

436

Table 2. $TkR99D^{RNAi}$ in insulin-producing cells blocks increased expression of *dilp3* and *dilp5*, but not *dilp2*, by *A. pomorum*: *post-hoc* tests.

Transcript	contrast	estimate	SE	df	t.ratio	p.value
dilp2	(axenic -) - (ap -)	0.34	0.82	24	0.42	0.98
	(axenic -) - (axenic +)	0.05	0.82	24	0.06	1
	(axenic -) - (ap +)	1.15	0.82	24	1.4	0.51
	(ap -) - (axenic +)	-0.29	0.82	24	-0.35	0.98
	(ap -) - (ap +)	0.81	0.82	24	0.98	0.76
	(axenic +) - (ap +)	1.1	0.82	24	1.34	0.55
dilp3	(axenic -) - (ap -)	-3.9	0.82	24	-4.74	0.0004
	(axenic -) - (axenic +)	-2.67	0.82	24	-3.24	0.02
	(axenic -) - (ap +)	-0.93	0.82	24	-1.13	0.67
	(ap -) - (axenic +)	1.23	0.82	24	1.5	0.45
	(ap -) - (ap +)	2.97	0.82	24	3.6	0.01
	(axenic +) - (ap +)	1.73	0.82	24	2.1	0.18
dilp5	(axenic -) - (ap -)	-4.18	0.82	24	-5.07	0.0002
	(axenic -) - (axenic +)	-3.32	0.82	24	-4.03	0.003
	(axenic -) - (ap +)	-1.19	0.82	24	-1.45	0.48
	(ap -) - (axenic +)	0.86	0.82	24	1.04	0.73
	(ap -) - (ap +)	2.98	0.82	24	3.62	0.01
	(axenic +) - (ap +)	2.13	0.82	24	2.58	0.07

437

438

439 Finally, we tested whether *TkR99D*^{RNAi} in IPCs blocked lifespan shortening by *A. pomorum* (Figures
440 7G-H). As expected, without *TkR99D*^{RNAi}, *Ap*-flies were shorter-lived than axenics. *TkR99D*^{RNAi}
441 induction in IPCs did not affect axenic lifespan but, surprisingly, the lifespan-shortening effect of *A.*
442 *pomorum* was exaggerated by *TkR99D*^{RNAi} induction (Figure 7H). Consequently, *A. pomorum's* effect
443 on lifespan seemingly cannot be explained by TkR99D activation in IPCs. We also tested whether
444 *TkR99D*^{RNAi} in IPCs altered effects of *A. pomorum* on TAG levels in young flies (Figure 7I): no interaction
445 was apparent (though we detected independent effects of microbiota (ANOVA F=14.95, Df=1,37,
446 p=0.0004) and RNAi induction (F=4.32, Df=1,37, p=0.04)), suggesting that interactive effects of *A.*
447 *pomorum* and Tk peptides are not mediated by *TkR99D* in IPCs.
448
449 Altogether, these data outline involvement of insulin signalling in responses to *A. pomorum* and *Tk*,
450 because IPC ablation blocked lifespan shortening by *A. pomorum* (Figure 7D-E), and because *dFoxO*
451 was required for the interaction of *A. pomorum* and *Tk*^{RNAi}. However, the failure of *TkR99D*^{RNAi} in IPCs
452 to block *A. pomorum's* effects on lifespan or TAG suggests that insulin signalling does not act
453 downstream of the putative *A. pomorum*/Tk/TkR signalling relay. These data may suggest priming, with
454 insulin signalling required to potentiate responses to *A. pomorum*/Tk/TkR.
455

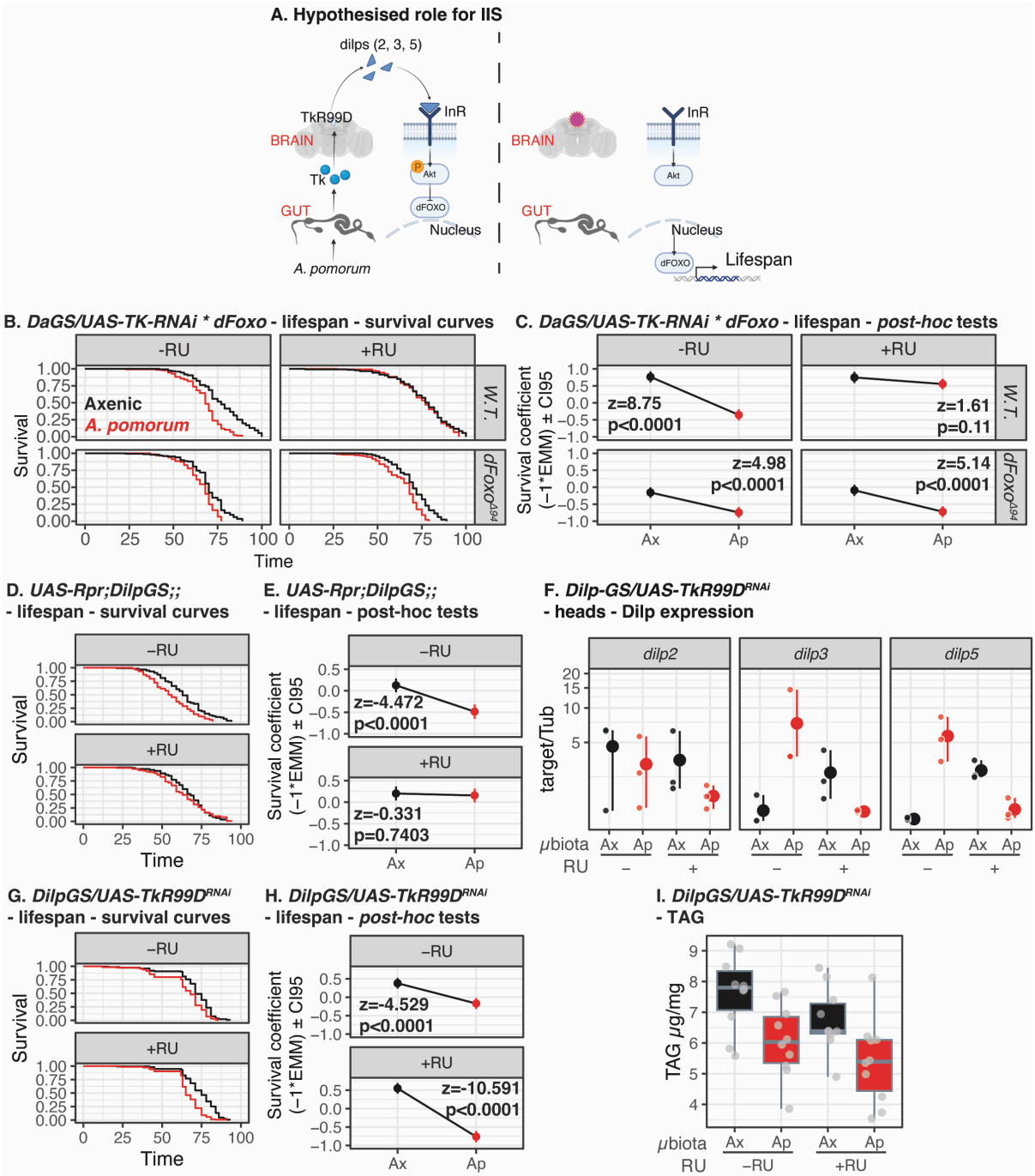

Figure 7. Insulin signalling is involved in lifespan response to *A. pomorum* and *TkR99D* knockdown, but not obligately required. A. Hypothetical model of role for insulin signalling. In presence of microbiota (left), Tk peptides are released from gut and contact TkR99D in IPCs/brain. IPCs are released into circulation, activating insulin signalling in peripheral tissues and leading to nuclear exclusion of dFOXO. In absence of microbiota (right), extracellular signalling is diminished, reducing downstream insulin signalling and consequent activation of lifespan-extending gene expression program by dFOXO. **B.** dFOXO connects lifespan responses to *A. pomorum* and ubiquitous *Tk*^{RNAi}. Facets show Kaplan-Meier plots in axenic and *A. pomorum* conditions, with/without RNAi induction (RU), and with/without *dFoxO*$^{\Delta 94}$ null mutation**.** Overall microbiota*RU*Foxo interaction p=5.384e-05 (CoxPH). All conditions n=150 except W.T. *A. pomorum* -RU (n=135) and W.T. axenic

467 +RU (n=148). **C.** Post-hoc comparisons (EMmeans), showing impact of *A. pomorum* under specified
468 conditions of *TkRNAi* induction and *dFoxO* deletion. *A. pomorum* shortens wild-type lifespan, but this
469 effect is diminished by *dFoxO*$^{\Delta 94}$. *Tk*^{RNAi} induction blocks lifespan shortening by *A. pomorum* in wild-
470 type background, but not in *dFoxO*$^{\Delta 94}$ background; altogether suggesting that *dFoxO* is required for *A.*
471 *pomorum* to influence longevity via Tk modulation. **D-E.** Insulin-producing cells (IPCs) are required for
472 *A. pomorum* to influence lifespan (CoxPH p=0.003). All conditions n=120. Post-hoc tests (**E**) confirm
473 that lifespan effect of *A. pomorum* (-RU) is absent following IPC ablation (*Rpr* expression, +RU). **F.** *A.*
474 *pomorum* increases expression of *Dilp3* and *Dilp5,* but not *Dilp2*, in a *TkR99D* -dependent manner.
475 Panels show expression (RT-qPCR) in heads of axenic and *Ap*-flies ±*TkR99D*^{RNAi} in IPCs (*Dilp2-*
476 *GS/UAS-TkR99D*^{RNAi}). by Microbiota*RU interactions were tested for with linear models: *Dilp2*
477 $F_{1,24}$=0.424, p=0.5, *Dilp3* $F_{1,24}$=23.404, p=0.0001, *Dilp5* $F_{1,24}$=29.261, p<0.0001. **G-H.** *TkR99D*^{RNAi} in
478 IPCs worsens lifespan impact of *A. pomorum*. Ap -RU n=160, Ap +RU n=162, Ax -RU n=160, Ax +RU
479 n=163. (**I**) Post-hoc tests indicate accentuated shortening of lifespan by *A. pomorum* following
480 *TkR99D*^{RNAi} induction (+RU). **I.** *TkR99D*^{RNAi} in IPCs does not modulate metabolic impact of *A. pomorum*
481 on fly TAG. The two experimental factors each had significant effects on TAG (ANOVA, *A. pomorum*
482 F=14.95, Df=1,37, p=0.0004; RU F=4.32, Df=1,37, p=0.04), but no interaction was detected.
483
484 **No evidence of role for *TkR99D* in Akh-producing cells in lifespan and metabolic response to *A.***
485 ***pomorum***
486 In insects, adipokinetic hormone (Akh) is released from *corpora cardiaca* (cc) to promote lipid
487 mobilisation in response to heightened energy demand, analogous to glucagon in mammals (Gäde and
488 Marco, 2022; Musselman et al., 2018; Toprak et al., 2020). Having observed *Tk*-dependent effects of
489 microbiota on TAG storage, and following recent evidence that *TkR99D* in Akh-producing cells limits
490 lifespan (Ahrentløv et al., 2025) , we tested whether it may also mediate lifespan impact of *A. pomorum*.
491
492 First, to test whether Akh peptide levels in CC were *A. pomorum*-dependent, we quantified Akh with
493 antibody staining. Akh staining levels were significantly higher in CC dissected from *Ap*-flies than
494 axenics (Figure 8A), suggesting microbial regulation of Akh signalling.
495
496 We then tested directly whether TkR99D was required in Akh-producing cells for *A. pomorum* to shorten
497 lifespan. *A. pomorum* shortened lifespan across the all different *Akh* conditions (Figure 8B-C).
498 Expressing *TkR99D*^{RNAi} under control of *Akh-Gal4* did extend lifespan in both axenics and *Ap*-flies,
499 corroborating a recent report of the CC's role in longevity (Ahrentløv et al., 2025) (noting background
500 effects, despite backcrossing immediately before experimentation) (Figure 8B-C). However, these data
501 indicate that lifespan shortening by *A. pomorum* is independent of TkR99D in CC. We also tested
502 whether RNAi against Akh receptor (*AkhR*) in adipose (fat body) altered response to *A. pomorum*,
503 driving expression with *S106-GS*, but again no interaction was apparent (Figure S10). Finally, we tested
504 whether *TkR99D* in Akh-producing cells interacted with effects of *A. pomorum* on TAG storage.
505 *TkR99D*^{RNAi} induction did not block response to *A. pomorum*, with *Ap*-flies storing less lipid than axenics

506 independent of fly genotype (Figure 8D), indicating that *A. pomorum*'s influence on TAG does not
507 depend on TkR99D in CC. Combined with our investigation of insulin signalling, our studies of Akh
508 suggest that the impact of *Acetobacter* on ageing is mediated by non-canonical mechanisms that
509 depend on *Tk* and *TkR99D.*
510

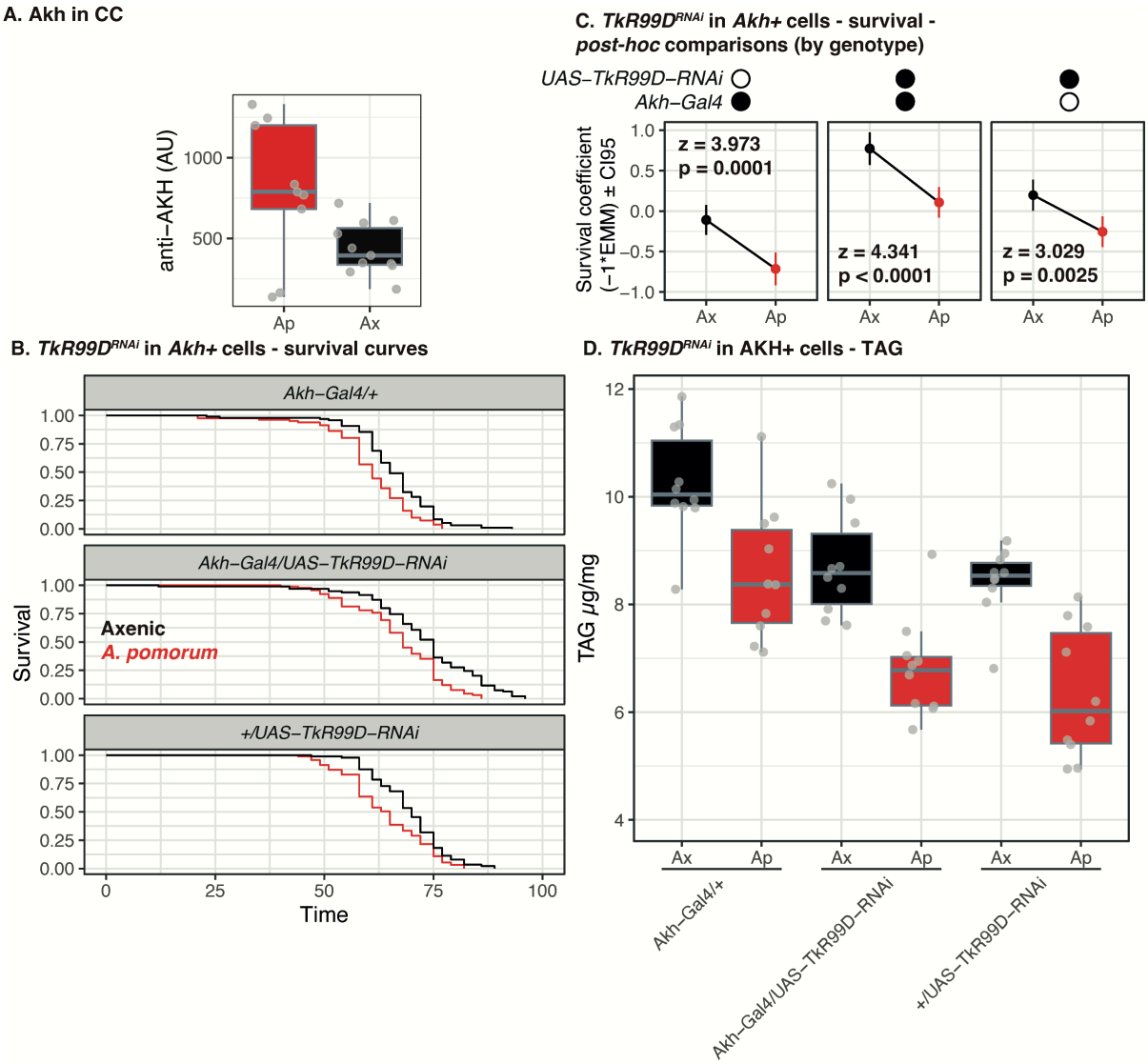

511
512 **Figure 8. *A. pomorum* modulation of host lifespan and TAG is independent of *TkR99D* in Akh-**
513 **producing cells. A.** Antibody staining of Akh in dissected Corpora Cardiaca (CC) is increased in *Ap*-
514 flies (Ap) relative to axenics (Ax). (t-test: t = -2.36, p-value = 0.04). **B.** Microbial shortening of lifespan
515 is independent of *TkR99D* signalling in Akh+ cells. Facets show Kaplan-Meier survival curves for axenic
516 and *Ap*-flies when *TkR99D* is knocked down (middle facet) and in each control genotype. No significant
517 interaction of genotype and *A. pomorum* was detected (CoxPH p=0.58). *Akh-Gal4/+ A. pomorum*
518 n=103, *Akh-Gal4/+* axenic n=108, *Akh-Gal4/UAS-TkR99D-RNAi A. pomorum* n=105, *Akh-Gal4/UAS-*
519 *TkR99D-RNAi* axenic n=107, *+/UAS-TkR99D-RNAi A. pomorum* n=103, *+/UAS-TkR99D-RNAi* axenic
520 n=101. **C.** Post-hoc comparisons (EMmeans) confirm equivalent lifespan shortening by *A. pomorum*,
521 independent of *TkR99D*^{RNAi}. Combination of transgenes indicated above facets. **D.** *A. pomorum*

522 modulation of host TAG is independent of *TkR99D*^{RNAi} in Akh+ cells. Boxplots show TAG levels are
523 reduced independent of *TkR99D*^{RNAi} induction. No significant interaction of genotype and *A. pomorum*
524 detected.
525
526

527

528 ## Discussion

529 Microbiota impact ageing across animals (Cabreiro et al., 2013; Cui et al., 2019; Sannino et al., 2018;
530 Seidel and Valenzano, 2018; Smith et al., 2017; Snyder et al., 1990; Tazume et al., 1991), and
531 connections between gut and the nervous system are key to health throughout the lifecourse (Boehme
532 et al., 2022; Dinan and Cryan, 2017; Qansuwa et al., 2024). Here we have connected microbial
533 regulation of ageing with tissue-specific regulation of endocrine signalling genes in gut and neurons.
534 Our *Drosophila* results show that (A) *A. pomorum* is sufficient to modulate *Tk* in the midgut, (B) knocking
535 down the peptide in midgut blocks the lifespan response to the bacteria, and (C) neuronal knockdown
536 of the receptor *TkR99D* recapitulates these effects. We are struck by the specificity of this circuit, with
537 knockdown of a single peptide-encoding locus in a specific tissue ablating the microbial impact on
538 lifespan, despite the wide array of host functions that the microbiota affect. This specific requirement
539 can likely be explained by the highly pleiotropic functions of Tachykinins (Nässel, 2025; Nässel et al.,
540 2019), suggesting that *Tk* knockdown reprograms organismal physiology to a state in which lifespan
541 can no longer be modulated by microbiota. Given the evolutionary conservation of tachykinins, it will be
542 interesting in future work to ask whether this family of peptides can also modulate ageing in other
543 species.

544

545 Our work indicates that the influence of the microbiota-*Tk/TkR99D* relay is partially independent of
546 better-studied lifespan assurance mechanisms, i.e. insulin signalling, and phenotypes associated with
547 ageing. The lifespan benefit of *Tk* knockdown was not accompanied by costs to fecundity or feeding
548 rate in CR flies, but instead knockdown altered metabolic impact of microbiota. Furthermore, knocking
549 down *TkR99D* in major signalling hubs associated with ageing and TAG metabolism (IPCs and Akh+
550 cells, respectively) did not block lifespan or TAG response to *A. pomorum*, suggesting that yet-
551 uncharacterised neuroendocrine mechanisms are at play. We interpret the partial requirement for
552 *dFoxO*, connecting *A. pomorum* to Tk^{RNAi} modulation of lifespan, as suggesting that insulin potentiates
553 downstream responsiveness, without necessarily being involved directly by *TkR99D* in IPCs.

554

555 Our work was performed entirely in females. We chose to study the sex that tends to exhibit more robust
556 response to anti-ageing interventions (Regan and Partridge, 2013) , because of the labour-intensive
557 and technically challenging nature of performing lifespan experiments under lifelong axenic conditions.
558 Having established this the *A. pomorum-Tk-TkR99D* connection, it will be interesting in future work to
559 ask whether males also enjoy a lifespan benefit of diminishing the activity of this circuit.

560

561 *Tk* is one of a number of signalling circuits implicated downstream of the microbiota, for example JAK-
562 STAT and JNK signalling (Buchon et al., 2009), IMD (Jugder et al., 2021; Watnick and Jugder, 2020),
563 and the neuropeptide CNMamide (Kim et al., 2021). We do not propose that Tachykinins alone are
564 sufficient to explain all physiological effects of the microbiota: rather we expect that the interplay of

565 multiple signalling pathways collectively orchestrate the host organismal response to microbiota. Indeed
566 our transcriptome (re)analysis (Figure 1B) suggested that a community of bacteria co-regulate
567 expression of the neuropeptides *ITP, AstC* and *NPF* alongside *Tk.* We note that *Tk* and *NPF* are co-
568 expressed in a number of the same EE populations (Guo et al., 2019), and related functions on nutrient-
569 specific appetite, physiology and Akh signalling are reported (Ahrentløv et al., 2025; Malita et al., 2022) ,
570 suggesting closely coupled functions for Tk and NPF which may also be relevant to integrating
571 responses to microbiota. Further work should aim to identify the broader signalling networks that
572 respond to the microbiota, and the extent to which the constituents and structure of those networks
573 mirror what is known in other contexts (e.g. responses to diet or pathogenic infection).
574
575 A key element to better understanding how signalling networks at large respond to microbiota will be to
576 better understand what properties of the microbiota the signals convey. Signalling is selected to convey
577 information about environmental, nutritional, and physiological state: which of these parameters do the
578 microbiota impact? Impacts on metabolism could be mediated by direct provision of nutrients (e.g.
579 short-chain fatty acids, B-vitamins (Sannino et al., 2018; S. C. Shin et al., 2011; A. C.-N. Wong et al.,
580 2014)), and/or competition with the host by removal of nutrients from diet (Huang and Douglas, 2015).
581 Immunity may be modulated by bacterial titre, to prevent pathological overgrowth of otherwise
582 mutualistic bacteria. Our results indicate that the interplay between bacteria and *Tk* knockdown is
583 bacteria-specific, suggesting in turn that more complex mixes of bacteria that co-occur with the fly may
584 elicit distinct signalling network topologies. Furthermore, the previous finding that fly transcriptional
585 networks are structured by microbiota (Dobson et al., 2016) leads to a question of whether other host
586 networks - such as endocrine signalling - may also be structured by microbiota, in which case signalling
587 in the presence of one bacterium might elicit quite different physiological responses than in the presence
588 of a distinct bacterium.
589
590 The two biggest mechanistic questions arising from this work are (A) from where in the nervous system
591 does *TkR99D* inhibition extend lifespan? and (B) by what mechanism does inhibition extend lifespan?
592 We tested two neuroendocrine tissues, the IPCs and the Akh+ cells, finding that $TkR99D^{RNAi}$ in either
593 did not block shortened lifespan or TAG phenotypes in *Ap*-flies (though bacteria-independent effects of
594 $TkR99D^{RNAi}$ in *Akh+* cells were apparent). These data suggest that we can reject a role for TkR99D in
595 IPCs and *Akh+* cells, and instead that an elusive population of *TkR99D+* neurons is at play downstream
596 of the *Acetobacter-Tk* relay. With respect to future mechanistic understanding, we suggest it will be
597 important to note that pan-neuronal $TkR99D^{RNAi}$ also mitigated gut permeability (smurfing) in aged *Ap*-
598 fies, because the smurf phenotype is underpinned by increased immune system activity (Clark et al.,
599 2015; Clark and Walker, 2017) , and activation of *Tk* cells by *Acetobacter* is dependent on immune
600 (IMD) signalling (Jugder et al., 2021). Together these observations suggest close links between *Tk*
601 signalling and immunity, outlining a possible role for *Acetobacter/Tk/TkR99D* in "inflammaging".
602

603 The biggest comparative question arising from our work is whether our findings are relevant in other
604 animals, potentially including mammals. Flies have a track record of revealing mechanisms of ageing
605 that are conserved in other systems (Bjedov et al., 2010; Clancy et al., 2001; Harrison et al., 2009;
606 Kenyon et al., 1993; Miller et al., 2014; Selman et al., 2008; Wilkinson et al., 2012; Zhang et al., 2024).
607 Tachykinins are conserved from invertebrates to mammals, raising the question of whether their
608 functions in ageing are also conserved. The next step would most likely be to assess whether
609 Tachykinin knockdown has anti-ageing effects in rodents, and/or short-lived vertebrates like the African
610 turquoise killifish. Such studies may pave the way for drug repurposing, as some small-molecule
611 inhibitors of human TkRs have already been developed and are licenced in some jurisdictions for
612 specific purposes. Such interest is timely since the therapeutic role of TkRs is receiving renewed
613 attention for potential metabolic therapies (Sass et al., 2024).
614
615 In conclusion, our study establishes a mechanistic connection between the microbiota and ageing via
616 gut/neuron signalling. Microbial shortening of host lifespan depends on *Tk/TkR* signalling, which can be
617 explained by *Acetobacter* activating intestinal *Tk* and, downstream, neuronal *TkR99D*. The findings hint
618 at effects which may be conserved in other systems, which may ultimately help to explain
619 mechanistically why microbiota exert a conserved influence on animal health and ageing.
620

621 ## Materials and methods

622

623 **Flies, bacteria, husbandry and culturing**

624 Stocks used are detailed in Table 3. All stocks (except for recombinant *R57C10-Gal80;;Tk-T2A-Gal4,*
625 gift from Kim Rewitz) were backcrossed into the Dahomey background (originally isolated from Benin
626 in the 1970s), bearing the *w1118* mutation and confirmed *Wolbachia*-negative. Presence of $dFoxO^{\Delta 94}$
627 in recombinant flies was confirmed by PCR of mothers of single-fly crosses.

628 All flies were maintained at 25°C with a 12-12-hour light- dark cycle on SYA medium, comprising 5%
629 sucrose (MP Biomedicals BP220), 10% yeast (MP Biomedicals, 903312, lot no. S7760), and 1.5% agar
630 (Sigma-Aldrich A7002)(Bass et al., 2007; Sannino and Dobson, 2023). Preservatives (0.3% nipagin,
631 0.3% propionic acid) were incorporated into media for stock maintenance. Crosses were performed on
632 juice agar in egg laying cages (per litre: 20g agar, 26g sucrose, 52g glucose, 7g yeast, 88.8ml organic
633 clementine or grape juice). To generate axenic flies, eggs were collected and washed 2x in alternating
634 10% bleach for (3-5 min) and sterile ddH2O for (1 min), with an optional additional 1 min wash in EtOH,
635 before being allowed to pellet by gravity in sterile PBS. 20 μl of egg pellet was aspirated with wide-
636 mouthed pipette tips into T75 flasks containing 50mL SYA. Preservatives were included during fly
637 development only in CR experiments. We made gnotobiotic embryos as as previously (Sannino and
638 Dobson, 2023). M9+lactate media comprised 200ml 5x M9 salts, 2ml 1M $MgSO_4$, 1ml 1M $CaCl_2$, 25ml
639 20% (v/v) lactate, made up to 1l in ddH_2O and autoclaved. YPD media comprised 10g yeast extract

640 (VWR 84601.0500), 20g peptone (VWR 84620.0500), 20g dextrose (Fisher Life Sci G/0500/53).
641 *Acetobacter pomorum* (DmCS004) was streaked and grown on M9+lactate plates (1.5% agar), before
642 growing single colonies in liquid M9+lactate at 30°C with shaking (225 rpm) for 2 days. (DmCS004). *L.*
643 *brevis* (DmCS003) was streaked on YPD (1.5% agar), then grown in liquid YPD for two days at 30C in
644 static culture. Cultures were pelleted, washed, resuspended and diluted in sterile PBS to an OD_{600} of
645 0.2. 200 μL of bacterial suspensions were added to T75 flasks containing freshly-prepared axenic eggs.

646 Newly emerged flies transferred to fresh media using sterile technique in a laminar flow hood,
647 (preservatives as per development) for the first three days of adulthood before gentle anaesthesia on
648 CO_2. Males were removed and females allocated to SYA containing preservatives in sterile glass
649 *Drosophila* vials, using aseptic technique in a laminair flow hood with a sterile paint brush and sterile
650 petri dish on ice. In experiments using RU486 (Mifepristone, Cayman Chemical, CAY10006317), 2ml l^{-}
651 ^{1} of 100mM RU486 stock solution in EtOH was incorporated into media at 200μM final concentration,
652 and fed from day 3 adulthood onwards. 2ml EtOH was incorporated as vehicle control in RU-free
653 controls.

654 For lifespan assays, mated females were allocated to sterile glassware in groups of 15, and transferred
655 to fresh food every 2–3 days. At each transfer, deaths and censors were scored until all flies were dead.
656 For axenic and gnotobiotic lifespans, fly tipping was performed in a sterile laminar flow hood with aseptic
657 technique.
658

659 **Table 3. *Drosophila* stocks used in this study.**

Genotype	Abbreviation	Source		
		BDSC	VDRC	Other
		***UAS* lines**		
UAS-TK-shRNAi			v330743	
UAS-TK-RNAi		B25800		
UAS-TK-RNAi			v103662	
UAS-TkR99D-RNAi			v44369	
UAS-TkR86C-RNAi			v107090	
UAS-Reaper				Cathy Slack, U. Warwick
UAS-AkhR-RNAi				Kenneth Halberg, U. Copenhagen
UAS-MCD8::GFP				Julia Cordero, U. Glasgow
		***Gene Switch* drivers**		
Daughterless-GeneSwitch;	*DaGS*			Cathy Slack, U. Warwick
Dilp2-GeneSwitch	*Dilp-GS*			Nathan Woodling, U. Glasgow
S106-GeneSwitch	*S106-GS*			Cathy Slack, U. Warwick
Elav-GeneSwitch	*Elav-GS*			Nathan Woodling, U. Glasgow
Mex-GeneSwitch	*Mex-GS*			Jean-René Martin, CNRS Université Paris-Saclay

	***GAL4* drivers**	
Voila-GAL4		Julia Cordero, U. Glasgow
Akh-GAL4		Kenneth Halberg, U. Copenhagen
TK-T2A-GAL4	*TK-GAL4*	Kim Rewitz, U. Copenhagen
Chat-Gal80		Julia Cordero, U. Glasgow
R57C10-Gal80		Kim Rewitz, U. Copenhagen
	Other	
FoxO $^{\Delta}$		Cathy Slack, U. Warwick
White Dahomey-20	*wD*$^{-20}$	Enric Ureña & Nazif Alic, UCL.

660

661 **Feeding and egg laying assays**

662 Feeding rate was measured by quantifying average proboscis extension rate (PER) over 3-4 hours.
663 Vials containing 5 mated females each were arranged on a benchtop in a 25ºC room the night before
664 behavioural observations to allow acclimation. Experimenters were blinded to vial ID and experimental
665 condition. The following morning, PER was recorded by iteratively counting the instantaneous number
666 of flies feeding per vial for 3-4 hours. The average of these measurements per each given vial was
667 taken as that vial's feeding rate. At the end of the experiment, flies were disposed, and vials frozen. The
668 next day eggs were counted from the same frozen vials.

669 **TAG assay**

670 Female flies were collected and divided into groups of 5, 3 days post eclosion. Each group was weighed
671 on a Thermo microbalance to an accuracy of .01 mg. Weighed females were added to a sterile 2mL
672 screw-cap tube containing sterile 1.4mm ceramic beads and 125 μL of TET buffer (10mM Tris, 1mM
673 EDTA, pH 8.0, 0.1% (v/v) Triton-X-100). Samples were homogenised for 30s at max speed. After
674 homogenisation, samples were incubated at 72°C for 15 min in a dry bath to inactivate lipases and
675 other enzymes. Then samples were centrifuged at max speed for 5 min at 4°C. From each sample 3
676 μL of the supernatant was added to a clear, flat bottom 96 well plate. Standard curves were generated
677 using a glycerol stock ranging from 1-0 ug/ul. Triglyceride levels were assayed by the method of Fossati
678 and Prencipe(Fossati and Prencipe, 1982) , with absorbance measured at 540 nm in a Thermo
679 MultiSkan FC plate reader.

680 **RNA extraction**

681 RNA was extracted from whole flies by the addition of 10 female flies per sample to sterile 2 mL screw
682 cap tubes containing 600 μL of TRIzol (Ambion by Life technologies) and homogenised in a Ribolyzer
683 and running at 6.5 (max) for 10 seconds. 200 μL chloroform was added, briefly vortexed, and incubated
684 at RT for 3 min. Samples were centrifuged 12,000rpm for 15m at 4ºC, 250μl of isopropanol was added
685 to supernatants, vortexed, and incubated at RT for 10 minutes. Samples were then centrifuged at

686 12,000rpm for 10m at 4ºC. The liquid was removed and discarded, while the pellet containing the RNA
687 was washed with 1mL of 75% ethanol. Samples were centrifuged at 12,000 rpm for 10m at 4ºC. The
688 liquid was removed without disturbing the pellet, and the tubes were dried at RT with caps opened.
689 Pellets were reconstituted in DEPC water (10*µ*l/fly) and stored at -80ºC.
690
691 **16s amplicon sequencing**
692 DNA was extracted from whole guts, dissected from 3 day-old wild-type stock females (i.e.
693 conventionally-reared and bearing a complete microbiota, 5 per sample, 10 samples total) after 1
694 minute surface-sterilisation in 70% EtOH. Guts were deposited immediately into TRIzol and
695 homogenised in a ribolyser. 300*µ*l chloroform was added and inverted followed by 3 mins incubation at
696 room temperature, 15 minutes centrifugation at 12000g. Aqueous layer was removed before 500*µ*l back
697 extraction buffer (4M Guanidine thiocyanate, 50 mM sodium citrate, 1M Tris base) was added and
698 mixed by inverting. Samples were spun again at 12000g for 30 minutes and aqueous phase transferred
699 to new tubes with 400 *µ*l isopropanol. Samples were mixed by inversion, centrifuged 15 minutes at
700 12000g. Pellets were washed in 70% ethanol, dried, and resuspended in 50 *µ*l TE buffer.
701
702 Library prep was performed by the University of Glasgow MVLS Shared Research Facility from 12.5ng
703 input DNA per sample, with an initial PCR using Accustart PCRToughMix and 0.5*µ*l 10mM primers
704 against 16s V3/V4 region (FWD
705 TCGTCGGCAGCGTCAGATGTGTATAAGAGACAGCCTACGGGNGGCWGCAG, REV
706 GTCTCGTGGGCTCGGAGATGTGTATAAGAGACAGGACTACHVGGGTATCTAATCC), using 25
707 cycles at an annealing temperature of 60ºC, followed by barcoding with Illumina Nextera XT 1 primers,
708 cleanup with 0.9X Spri Select beads (Beckman Coulter), and washing in 80% EtOH. Libraries were
709 quantified by Qubit HS DNA assay and size distributions checked on an Agilent Bioanalyser. Pooled
710 libraries were sequenced on an Illumina MiSeq in paired end mode (300bp) using a 600 cycle cartridge
711 kit, 5% PhiX, to an average depth of 170K reads per sample.
712
713 **RT-qPCR**

714 RNA samples were quantified by spectrophotometry using a Nanodrop 1000 UV-Vis spectrophotometer
715 (ThermoScientific). First strand synthesis of cDNA was performed using the SuperScriptTM Reverse
716 Transcriptase (RT) kit (Invitrogen), following the manufacturer's protocol (using 2*µ*g of RNA). The PCR
717 profile was as follows: 95°C for 2 minutes; 94°C denaturation for 30 seconds, 60°C annealing for 30
718 seconds, 72°C extension for 30 seconds each for 40 cycles, with a final extension at 72°C for 5 minutes.
719 The amplicon was migrated through a 1% (w/v) agarose gel. To test for relative gene expression levels,
720 RT-qPCR was performed. Each well contained 2 µl cDNA, 1.5 µl 10 mM forward primer, 1.5 µl 10 mM
721 reverse primer, 3 µl water, 10 µl SYBR green PCR master mix, and 2 ul ROX (Qiagen, UK). The
722 following PCR profile was used: 95°C for 5 minutes; 94°C for 30 seconds, 60°C for 30 seconds, 72°C
723 for 30 seconds each for 40 cycles, and a final extension at 72°C for 5 minutes. Mean cycle threshold

724 (Ct) values for duplicates of each of the studied genes were derived by subtracting the combined mean
725 Ct value of constitutively expressed housekeeping genes *alcohol dehydrogenase* (*ADH*) or *tubulin*.
726 Primers shown in Table 4.

727

728

729 **Table 4 Primers for RT-qPCR**

Target	*Forward*	*Reverse*
TK	TTCATATGCGCCCTCTGAGCG	ATGAAGCTGGACGTGGGCGC
Bursicon	CGCCACGAGAACAACAAGGT	CATCCAGGATACTGGAGCAC
ADH	GCTAACGAGTACTTGCATCTCTTC	AGACCGGCAACGAAAATCAC
Tubulin	TCGCCGTCACCGGAGTCCAT	TGGGCCCGTCTGGACCACAA
Dilp2	ATGGTGTGCGAGGAGTATAATCC	TCGGCACCGGGCATG
Dilp3	AGAGAACTTTGGACCCCGTGAA	TGAACCGAACTATCACTCAACAGTCT
Dilp5	GAGGCACCTTGGGCCTATTC	CATGTGGTGAGATTCGGAGCTA

730

731 **Antibody staining and imaging**

732 Whole guts were extracted from 10-day old female flies (axenic, gnotobiotic, and axenic on 1μM
733 TSA), and fixed in 4% paraformaldehyde for 30m in a 12 well plate. Guts were then incubated in 1 mL
734 of PBST (1X PBS with 0.1% triton X-100) overnight with slight shaking at 4ºC. PBST was carefully
735 aspirated from sample wells, and guts were then washed with 1 mL of Blocking buffer (10% 1X PBS,
736 1% triton X-100, 2.5% Normal Goat Serum) at 4ºC overnight. Blocking buffer was removed, and 0.5
737 mL of acetyl-lysine antibody (Cell Signaling Technologies 9441) diluted 1/800 in blocking buffer was
738 added to the wells, and incubated overnight at 4ºC with slight shaking. Guts were then washed 3X
739 with PBST for 10 minutes, followed by a 1 hr RT PBST wash with slight shaking. 0.5 mL of secondary
740 antibody secondary antibodies diluted 1/200 in PBST was added to the guts, and incubated overnight
741 at 4ºC. Guts were washed 3X in PBST for 10 minutes. Guts were then mounted in Vectashield for
742 imaging.

743 Corpora cardiaca were dissected, fixed and washed as above, stained with anti-Akh (gift from
744 Kenneth Halberg) diluted 1:1000, and stained with secondary antibodies as above.

745 **Confocal microscopy**

Imaging was performed on a Zeiss LSM 880 confocal microscope and processed using Zeiss Zen Blue (v3.8) and NIH ImageJ software 1.53a prior to transfer to Adobe Photoshop and Illustrator (Creative Cloud 2025; CA, USA) for final presentation.

Data analysis

All enumerated data were plotted and analysed in R 4.4.2. (Team, 2024). Kaplan-Meier curves were plotted with survminer::ggsurvplot_facet. Other quantitative data were plotted with ggplot2. Survival data were analysed with CoxPH models (survival::coxph). Fecundity data were analysed with negative binomial models (lme4::glmer.nb). All other data were analysed with stats::lm (after logit transformation for proportion flies feeding). Post-hoc tests were performed with emmeans::joint_tests and emmeans::pairs, coefficients were extracted from emmeans::emmip. Survival indices were generated by applying emmeans::emmip to coxph models, multiplied by -1, such that higher values corresponded to longer lifespan.

Published transcriptome data (Bost et al., 2018) were reanalysed by FastQC and quantified with Salmon. The previous publication by Bost et al(Bost et al., 2018) presented bulk RNAseq on midguts of flies reared under axenic conditions or with a 5-species gnotobiotic microbiota comprising *Acetobacter* and *Levilactobacillus* species. The original analysis presented excluded expression of ~70% of genes in the fly genome, and hormones were largely excluded. We reanalysed the raw data using Salmon (Patro et al., 2017) to quantify expression, which quantified expression of 10,290 genes, including 14 of the 15 enteroendocrine hormone genes (except *bursicon*). We tested for differential expression using DESeq2, identifying 470 differentially expressed genes (FDR ≤ 0.01, ≥2-fold difference in mean expression). These 470 genes included four peptide hormones: *Tachykinin (Tk), Allostatin C (AstC), Ion Transport Peptide (ITP), and Neuropeptide F (NPF).* Since *Burs* was not quantified by the Salmon algorithm, we tested independently whether its expression was modulated by microbiota by extracting RNA from midguts of CR and axenic flies.

Acknowledgments

We thank Julia Cordero for helpful discussion, reagents and training; Nathan Woodling and Colin Selman for comments on the manuscript; and Kim Rewitz, Kenneth Halberg, Jean-René Martin and Peter Newell for reagents. The authors gratefully acknowledge the Cellular Analysis Facility at the University of Glasgow – particularly David McGuinness – for support and assistance in this work. This work was funded by a UKRI Future Leaders Fellowship (MR/S033939/1 and MR/Y019660/1, AD), BBSRC (BB/W510658/1, DRS and AD), a University of Glasgow Lord Kelvin Adam Smith Fellowship (AD), a University of Glasgow Lord Kelvin Adam Smith Scholarship (RI), and funds from the University of Glasgow Wellcome Trust Institutional Strategic Support award (RI and AD).

Bibliography

Ahrentløv N, Kubrak O, Lassen M, Malita A, Koyama T, Frederiksen AS, Sigvardsen CM, John A, Madsen PEH, Halberg KV, Nagy S, Imig C, Richter EA, Texada MJ, Rewitz K. 2025. Protein-responsive gut hormone tachykinin directs food choice and impacts lifespan. *Nat Metab* **7**:1223–1245. doi:10.1038/s42255-025-01267-0

Alic N, Tullet JM, Niccoli T, Broughton S, Hoddinott MP, Slack C, Gems D, Partridge L. 2014. Cell-nonautonomous effects of dFOXO/DAF-16 in aging. *Cell reports* **6**. doi:10.1016/j.celrep.2014.01.015

Bass TM, Grandison RC, Wong R, Martinez P, Partridge L, Piper MDW. 2007. Optimization of Dietary Restriction Protocols in Drosophila. *Journals Gerontology Ser* **62**:1071–1081. doi:10.1093/gerona/62.10.1071

Birse RT, Söderberg JA, Luo J, Winther ÅM, Nässel DR. 2011. Regulation of insulin-producing cells in the adult Drosophila brain via the tachykinin peptide receptor DTKR. *The Journal of Experimental Biology* **214**:4201–4208. doi:10.1242/jeb.062091

Bjedov I, Toivonen J, Kerr F, Slack C, Jacobson J. 2010. Mechanisms of life span extension by rapamycin in the fruit fly Drosophila melanogaster.

Boehme M, Guzzetta KE, Wasén C, Cox LM. 2022. The gut microbiota is an emerging target for improving brain health during ageing. *Gut Microbiome* **4**:e2. doi:10.1017/gmb.2022.11

Bost A, Franzenburg S, Adair KL, Martinson VG, Loeb G, Douglas AE. 2018. How gut transcriptional function of Drosophila melanogaster varies with the presence and composition of the gut microbiota. *Mol Ecol* **27**:1848–1859. doi:10.1111/mec.14413

Broderick NA, Buchon N, Lemaitre B. 2014. Microbiota-induced changes in drosophila melanogaster host gene expression and gut morphology. *mBio* **5**:e01117-14. doi:10.1128/mbio.01117-14

Broughton SJ, Piper MD, Ikeya T, Bass TM, Jacobson J, Driege Y, Martinez P, Hafen E, Withers DJ, Leevers SJ, Partridge L. 2005. Longer lifespan, altered metabolism, and stress resistance in Drosophila from ablation of cells making insulin-like ligands. *Proceedings of the National Academy of Sciences of the United States of America* **102**:3105–3110. doi:10.1073/pnas.0405775102

Brown JJ, Jandová A, Jeffs CT, Higgie M, Nováková E, Lewis OT, Hrček J. 2023. Microbiome structure of a wild Drosophila community along tropical elevational gradients and comparison to laboratory lines. *bioRxiv* 2021.07.28.454263. doi:10.1101/2021.07.28.454263

Brummel T, Ching A, Seroude L, Simon AF, Benzer S. 2004. Drosophila lifespan enhancement by exogenous bacteria. *Proceedings of the National Academy of Sciences of the United States of America* **101**:12974–12979. doi:10.1073/pnas.0405207101

Buchon N, Broderick NA, Chakrabarti S, Lemaitre B. 2009. Invasive and indigenous microbiota impact intestinal stem cell activity through multiple pathways in Drosophila. *Genes & development* **23**:2333–44. doi:10.1101/gad.1827009

Cabreiro F, Au C, Leung K-Y, Vergara-Irigaray N, Cochemé HM, Noori T, Weinkove D, Schuster E, Greene N, Gems D. 2013. Metformin Retards Aging in C. elegans by Altering Microbial Folate and Methionine Metabolism. *Cell* **153**:228–239. doi:10.1016/j.cell.2013.02.035

820 Chandler JA, Lang JM, Bhatnagar S, Eisen JA, Kopp A. 2011. Bacterial Communities of Diverse
821 Drosophila Species: Ecological Context of a Host–Microbe Model System. *PLoS Genet*
822 **7**:e1002272. doi:10.1371/journal.pgen.1002272

823 Chatzispyrou IA, Held NM, Mouchiroud L, Auwerx J, Houtkooper RH. 2015. Tetracycline Antibiotics
824 Impair Mitochondrial Function and Its Experimental Use Confounds Research. *Cancer Res*
825 **75**:4446–4449. doi:10.1158/0008-5472.can-15-1626

826 Clancy DJ, Gems D, Harshman LG, Oldham S, Stocker H, Hafen E, Leevers SJ, Partridge L. 2001.
827 Extension of Life-Span by Loss of CHICO, a Drosophila Insulin Receptor Substrate Protein.
828 *Science* **292**:104–106. doi:10.1126/science.1057991

829 Clark RI, Salazar A, Yamada R, Fitz-Gibbon S, Morselli M, Alcaraz J, Rana A, Rera M, Pellegrini M,
830 Ja WW, Walker DW. 2015. Distinct Shifts in Microbiota Composition during Drosophila Aging
831 Impair Intestinal Function and Drive Mortality. *Cell reports* **12**:1656–67.
832 doi:10.1016/j.celrep.2015.08.004

833 Clark RI, Walker DW. 2017. Role of gut microbiota in aging-related health decline: insights from
834 invertebrate models. *Cellular and Molecular Life Sciences*. doi:10.1007/s00018-017-2671-1

835 Cui R, Medeiros T, Willemsen D, Iasi LNM, Collier GE, Graef M, Reichard M, Valenzano DR. 2019.
836 Relaxed Selection Limits Lifespan by Increasing Mutation Load. *Cell*.
837 doi:10.1016/j.cell.2019.06.004

838 Dinan TG, Cryan JF. 2017. Gut instincts: microbiota as a key regulator of brain development, ageing
839 and neurodegeneration. *J Physiol* **595**:489–503. doi:10.1113/jp273106

840 Dobson AJ, Chaston JM, Douglas AE. 2016. The Drosophila transcriptional network is structured by
841 microbiota. *BMC genomics* **17**:975.

842 Dobson AJ, Chaston JM, Newell PD, Donahue L, Hermann SL, Sannino DR, Westmiller S, Wong AC,
843 Clark AG, Lazzaro BP, Douglas AE. 2015. Host genetic determinants of microbiota-dependent
844 nutrition revealed by genome-wide analysis of Drosophila melanogaster. *Nature communications*
845 **6**:6312. doi:10.1038/ncomms7312

846 Flatt T. 2009. Ageing: Diet and longevity in the balance. *Nature* **462**:989–990. doi:10.1038/462989a

847 Fossati P, Prencipe L. 1982. Serum triglycerides determined colorimetrically with an enzyme that
848 produces hydrogen peroxide. *Clin Chem* **28**:2077–2080. doi:10.1093/clinchem/28.10.2077

849 Gäde G, Marco HG. 2022. The Adipokinetic Peptides of Hemiptera: Structure, Function, and
850 Evolutionary Trends. *Front Insect Sci* **2**:891615. doi:10.3389/finsc.2022.891615

851 Gagnon E, Mitchell PL, Manikpurage HD, Abner E, Taba N, Esko T, Ghodsian N, Thériault S, Mathieu
852 P, Arsenault BJ. 2023. Impact of the gut microbiota and associated metabolites on
853 cardiometabolic traits, chronic diseases and human longevity: a Mendelian randomization study. *J*
854 *Transl Med* **21**:60. doi:10.1186/s12967-022-03799-5

855 Good T, Tatar M. 2001. Age-specific mortality and reproduction respond to adult dietary restriction in
856 Drosophila melanogaster.

857 Gordon HA, Bruckner-Kardoss E, Wostmann BS. 1966. Aging in germ-free mice: life tables and
858 lesions observed at natural death. *Journal of gerontology* **21**:380–7.

859 Grandison RC, Piper MD, Partridge L. 2009. Amino-acid imbalance explains extension of lifespan by
860 dietary restriction in Drosophila. *Nature* **462**:1061–1064. doi:10.1038/nature08619

861 Guo X, Yin C, Yang F, Zhang Y, Huang H, Wang J, Deng B, Cai T, Rao Y, Xi R. 2019. The Cellular
862 Diversity and Transcription Factor Code of Drosophila Enteroendocrine Cells. *Cell Reports*
863 **29**:4172-4185.e5. doi:10.1016/j.celrep.2019.11.048

864 Harrison DE, Strong R, Sharp ZD, Nelson JF, Astle CM, Flurkey K, Nadon NL, Wilkinson JE, Frenkel
865 K, Carter CS, Pahor M, Javors MA, Fernandez E, Miller RA. 2009. Rapamycin fed late in life
866 extends lifespan in genetically heterogeneous mice. *Nature* **460**:392–395.
867 doi:10.1038/nature08221

868 Houthoofd K, Braeckman BP, Lenaerts I, Brys K, Vreese AD, Eygen SV, Vanfleteren JR. 2002.
869 Axenic growth up-regulates mass-specific metabolic rate, stress resistance, and extends life span
870 in Caenorhabditis elegans. *Experimental gerontology* **37**:1371–8.

871 Huang J-H, Douglas AE. 2015. Consumption of dietary sugar by gut bacteria determines Drosophila
872 lipid content. *Biology Letters* **11**:20150469. doi:10.1098/rsbl.2015.0469

873 Hung R-JJ, Hu Y, Kirchner R, Liu Y, Xu C, Comjean A, Tattikota SG, Li F, Song W, Sui SH, Perrimon
874 N. 2020. A cell atlas of the adult Drosophila midgut. *Proceedings of the National Academy of*
875 *Sciences of the United States of America*. doi:10.1073/pnas.1916820117

876 Johansen J, Atarashi K, Arai Y, Hirose N, Sørensen SJ, Vatanen T, Knip M, Honda K, Xavier RJ,
877 Rasmussen S, Plichta DR. 2023. Centenarians have a diverse gut virome with the potential to
878 modulate metabolism and promote healthy lifespan. *Nat Microbiol* **8**:1064–1078.
879 doi:10.1038/s41564-023-01370-6

880 Jugder B-E, Kamareddine L, Watnick PI. 2021. Microbiota-derived acetate activates intestinal innate
881 immunity via the Tip60 histone acetyltransferase complex. *Immunity* **54**:1683-1697.e3.
882 doi:10.1016/j.immuni.2021.05.017

883 Kenyon C, Chang J, Gensch E, Rudner A, Tabtiang R. 1993. A C. elegans mutant that lives twice as
884 long as wild type. *Nature* **366**:461. doi:10.1038/366461a0

885 Kim B, Kanai MI, Oh Y, Kyung M, Kim E-K, Jang I-H, Lee J-H, Kim S-G, Suh GSB, Lee W-J. 2021.
886 Response of the microbiome–gut–brain axis in Drosophila to amino acid deficit. *Nature* **593**:570–
887 574. doi:10.1038/s41586-021-03522-2

888 Kubrak O, Koyama T, Ahrentløv N, Jensen L, Malita A, Naseem MT, Lassen M, Nagy S, Texada MJ,
889 Halberg KV, Rewitz K. 2022. The gut hormone Allatostatin C/Somatostatin regulates food intake
890 and metabolic homeostasis under nutrient stress. *Nat Commun* **13**:692. doi:10.1038/s41467-022-
891 28268-x

892 Leader DP, Krause SA, Pandit A, Davies SA, Dow JAT. 2018. FlyAtlas 2: a new version of the
893 Drosophila melanogaster expression atlas with RNA-Seq, miRNA-Seq and sex-specific data.
894 *Nucleic Acids Res* **46**:D809–D815. doi:10.1093/nar/gkx976

895 Lin H-H, Kuang MC, Hossain I, Xuan Y, Beebe L, Shepherd AK, Rolandi M, Wang JW. 2022. A
896 nutrient-specific gut hormone arbitrates between courtship and feeding. *Nature* **602**:632–638.
897 doi:10.1038/s41586-022-04408-7

898 Liu X, Nagy P, Bonfini A, Houtz P, Bing X-L, Yang X, Buchon N. 2022. Microbes affect gut epithelial
899 cell composition through immune-dependent regulation of intestinal stem cell differentiation. *Cell*
900 *Reports* **38**:110572. doi:10.1016/j.celrep.2022.110572

901 Liu X, Zou L, Nie C, Qin Y, Tong X, Wang J, Yang H, Xu X, Jin X, Xiao L, Zhang T, Min J, Zeng Y, Jia
902 H, Hou Y. 2023. Mendelian randomization analyses reveal causal relationships between the
903 human microbiome and longevity. *Sci Rep* **13**:5127. doi:10.1038/s41598-023-31115-8

904 Mair W, Piper MD, Partridge L. 2005. Calories Do Not Explain Extension of Life Span by Dietary
905 Restriction in Drosophila. *PLoS Biology* **3**:e223. doi:10.1371/journal.pbio.0030223

906 Malita A, Kubrak O, Koyama T, Ahrentløv N, Texada MJ, Nagy S, Halberg KV, Rewitz K. 2022. A gut-
907 derived hormone suppresses sugar appetite and regulates food choice in Drosophila. *Nat Metab*
908 **4**:1532–1550. doi:10.1038/s42255-022-00672-z

909 Matthews MK, Wilcox H, Hughes R, Veloz M, Hammer A, Banks B, Walters A, Schneider KJ, Sexton
910 CE, Chaston JM. 2020. Genetic Influences of the Microbiota on the Life Span of Drosophila
911 melanogaster. *Appl Environ Microb* **86**. doi:10.1128/aem.00305-20

912 Medina AB, Perochon J, Johnson C, Polcowñuk S, Tian Y, Yu Y, Cordero JB. 2024. Neuroendocrine
913 Control of Intestinal Regeneration Through the Vascular Niche in Drosophila. *bioRxiv*
914 2024.09.10.612352. doi:10.1101/2024.09.10.612352

915 Miller RA, Harrison DE, Astle CM, Fernandez E, Flurkey K, Han M, Javors MA, Li X, Nadon NL,
916 Nelson JF, Pletcher S, Salmon AB, Sharp ZD, Roekel SV, Winkleman L, Strong R. 2014.
917 Rapamycin-mediated lifespan increase in mice is dose and sex dependent and metabolically
918 distinct from dietary restriction. *Aging Cell* **13**:468–477. doi:10.1111/acel.12194

919 Moullan N, Mouchiroud L, Wang X, Ryu D, Williams EG, Mottis A, Jovaisaite V, Frochaux MV, Quiros
920 PM, Deplancke B, Houtkooper RH, Auwerx J. 2015. Tetracyclines Disturb Mitochondrial Function
921 across Eukaryotic Models: A Call for Caution in Biomedical Research. *Cell Rep* **10**:1681–1691.
922 doi:10.1016/j.celrep.2015.02.034

923 Musselman LP, Kühnlein RP, Suarez RK, Hoppeler HH. 2018. Drosophila as a model to study obesity
924 and metabolic disease. *J Exp Biol* **221**:jeb163881. doi:10.1242/jeb.163881

925 Nässel DR. 2025. What Drosophila can tell us about state-dependent peptidergic signaling in insects.
926 *Insect Biochem Mol Biol* 104275. doi:10.1016/j.ibmb.2025.104275

927 Nässel DR, Zandawala M, Kawada T, Satake H. 2019. Tachykinins: Neuropeptides That Are Ancient,
928 Diverse, Widespread and Functionally Pleiotropic. *Front Neurosci* **13**:1262.
929 doi:10.3389/fnins.2019.01262

930 Newell PD, Chaston JM, Wang Y, Winans NJ, Sannino DR, Wong ACN, Dobson AJ, Kagle J,
931 Douglas AE. 2014. In vivo function and comparative genomic analyses of the Drosophila gut
932 microbiota identify candidate symbiosis factors. *Front Microbiol* **5**:576.
933 doi:10.3389/fmicb.2014.00576

934 Newell PD, Douglas AE. 2014. Interspecies Interactions Determine the Impact of the Gut Microbiota
935 on Nutrient Allocation in Drosophila melanogaster. *Appl Environ Microbiol* **80**:788–796.
936 doi:10.1128/aem.02742-13

937 Obata F, Fons CO, Gould AP. 2018. Early-life exposure to low-dose oxidants can increase longevity
938 via microbiome remodelling in Drosophila. *Nat Commun* **9**:975. doi:10.1038/s41467-018-03070-w

939 OToole P, Jeffery I. 2015. Gut microbiota and aging. *Science* **350**:1214–1215.
940 doi:10.1126/science.aac8469

941 Partridge L, Gems D, Withers DJ. 2005. Sex and Death: What Is the Connection? *Cell* **120**.
942 doi:10.1016/j.cell.2005.01.026

943 Patro R, Duggal G, Love MI, Irizarry RA, Kingsford C. 2017. Salmon provides fast and bias-aware
944 quantification of transcript expression. *Nat Methods* **14**:417–419. doi:10.1038/nmeth.4197

945 Pryor R, Norvaisas P, Marinos G, Best L, Thingholm LB, Quintaneiro LM, Haes WD, Esser D,
946 Waschina S, Lujan C, Smith RL, Scott TA, Martinez-Martinez D, Woodward O, Bryson K, Laudes
947 M, Lieb W, Houtkooper RH, Franke A, Temmerman L, Bjedov I, Cochemé HM, Kaleta C, Cabreiro
948 F. 2019. Host-Microbe-Drug-Nutrient Screen Identifies Bacterial Effectors of Metformin Therapy.
949 *Cell*. doi:10.1016/j.cell.2019.08.003

950 Qansuwa EM, Atalah HN, Abdelkader MS, Russell AE, Dakhlallah D, Brown CM. 2024. Handbook of
951 Neurodegenerative Disorders 17–41. doi:10.1007/978-981-99-7557-0_2

952 Regan JC, Khericha M, Dobson AJ, Bolukbasi E, Rattanavirotkul N, Partridge L. 2016. Sex difference
953 in pathology of the ageing gut mediates the greater response of female lifespan to dietary
954 restriction. *eLife* **5**:e10956. doi:10.7554/elife.10956

955 Regan JC, Partridge L. 2013. Gender and longevity: Why do men die earlier than women?
956 Comparative and experimental evidence. *Best Pr Res Clin Endocrinol Metab* **27**:467–479.
957 doi:10.1016/j.beem.2013.05.016

958 Rera M, Clark R, Walker D. 2012. Intestinal barrier dysfunction links metabolic and inflammatory
959 markers of aging to death in Drosophila. *Proceedings of the National Academy of Sciences* **109**.
960 doi:10.1073/pnas.1215849110

961 Rewitz K, Ahrentlov N, Kubrak O, Malita A, Koyama T, John A, Madsen P, Halberg K, Nagy S,
962 Texada M. 2024. Protein-responsive gut hormone Tachykinin directs food choice and impacts
963 lifespan in Drosophila. doi:10.21203/rs.3.rs-3837414/v1

964 Ronayne CT, Jackson TD, Bennett CF, Perry EA, Kantorovic N, Puigserver P. 2023. Tetracyclines
965 activate mitoribosome quality control and reduce ER stress to promote cell survival. *EMBO Rep*
966 **24**:e57228. doi:10.15252/embr.202357228

967 Sannino DR, Dobson AJ. 2023. Acetobacter pomorum in the Drosophila gut microbiota buffers
968 against host metabolic impacts of dietary preservative formula and batch variation in dietary yeast.
969 *Appl Environ Microbiol* **89**:e00165-23. doi:10.1128/aem.00165-23

970 Sannino DR, Dobson AJ, Edwards K, Angert ER, Buchon N. 2018. The Drosophila melanogaster Gut
971 Microbiota Provisions Thiamine to Its Host. *mBio* **9**. doi:10.1128/mbio.00155-18

972 Sass F, Ma T, Ekberg JH, Kirigiti M, Ureña MG, Dollet L, Brown JM, Basse AL, Yacawych WT, Burm
973 HB, Andersen MK, Nielsen TS, Tomlinson AJ, Dmytiyeva O, Christensen DP, Bader L, Vo CT,
974 Wang Y, Rausch DM, Kristensen CK, Gestal-Mato M, Panhuis WI het, Sjøberg KA, Kernodle S,
975 Petersen JE, Pavlovskyi A, Sandhu M, Moltke I, Jørgensen ME, Albrechtsen A, Grarup N, Babu
976 MM, Rensen PCN, Kooijman S, Seeley RJ, Worthmann A, Heeren J, Pers TH, Hansen T,
977 Gustafsson MBF, Tang-Christensen M, Kilpeläinen TO, Myers MG, Kievit P, Schwartz TW,
978 Hansen JB, Gerhart-Hines Z. 2024. NK2R control of energy expenditure and feeding to treat
979 metabolic diseases. *Nature* **635**:987–1000. doi:10.1038/s41586-024-08207-0

980 Schwarzer M, Makki K, Storelli G, Machuca-Gayet I, Srutkova D, Hermanova P, Martino ME,
981 Balmand S, Hudcovic T, Heddi A, Rieusset J, Kozakova H, Vidal H, Leulier F. 2016. Lactobacillus
982 plantarum strain maintains growth of infant mice during chronic undernutrition. *Science (New York,*
983 *NY)* **351**:854–7. doi:10.1126/science.aad8588

984 Scopelliti A, Cordero JB, Diao F, Strathdee K, White BH, Sansom OJ, Vidal M. 2014. Local Control of
985 Intestinal Stem Cell Homeostasis by Enteroendocrine Cells in the Adult Drosophila Midgut.
986 *Current Biology* **24**. doi:10.1016/j.cub.2014.04.007

987 Seidel J, Valenzano D. 2018. The role of the gut microbiome during host ageing. *F1000Research*
988 **7**:F1000 Faculty Rev-1086. doi:10.12688/f1000research.15121.1

989 Selman C, Lingard S, Choudhury AI, Batterham RL, Claret M, Clements M, Ramadani F, Okkenhaug
990 K, Schuster E, Blanc E, Piper MD, Al-Qassab H, Speakman JR, Carmignac D, Robinson ICA,
991 Thornton JM, Gems D, Partridge L, Withers DJ. 2008. Evidence for lifespan extension and
992 delayed age–related biomarkers in insulin receptor substrate 1 null mice. *Faseb J* **22**:807–818.
993 doi:10.1096/fj.07-9261com

994 Shin S, Kim S-H, You H, Kim B, Kim AC, Lee K-A, Yoon J-H, Ryu J-H, Lee W-J. 2011. *Drosophila*
995 Microbiome Modulates Host Developmental and Metabolic Homeostasis via Insulin Signaling.
996 *Science* **334**:670–674. doi:10.1126/science.1212782

997 Shin SC, Kim S-H, You H, Kim B, Kim AC, Lee K-A, Yoon J-H, Ryu J-H, Lee W-J. 2011. *Drosophila*
998 Microbiome Modulates Host Developmental and Metabolic Homeostasis via Insulin Signaling.
999 *Science* **334**:670–674. doi:10.1126/science.1212782

1000 Slack C, Alic N, Foley A, Cabecinha M, Hoddinott MP, Partridge L. 2015. The Ras-Erk-ETS-Signaling
1001 Pathway Is a Drug Target for Longevity. *Cell* **162**:72–83. doi:10.1016/j.cell.2015.06.023

1002 Slack C, Giannakou ME, Foley A, Goss M, Partridge L. 2011. dFOXO-independent effects of reduced
1003 insulin-like signaling in Drosophila. *Aging Cell* **10**:735–748. doi:10.1111/j.1474-9726.2011.00707.x

1004 Slagboom PE, Berg N van den, Deelen J. 2017. Phenome and genome based studies into human
1005 ageing and longevity: An overview. *Biochimica Et Biophysica Acta Mol Basis Dis* **1864**:2742–2751.
1006 doi:10.1016/j.bbadis.2017.09.017

1007 Smith P, Willemsen D, Popkes M, Metge F, Gandiwa E, Reichard M, Valenzano DR. 2017.
1008 Regulation of life span by the gut microbiota in the short-lived African turquoise killifish. *eLife* **6**.
1009 doi:10.7554/elife.27014

1010 Snyder D, Pollard M, Wostmann B, Luckert P. 1990. Life span, morphology, and pathology of diet-
1011 restricted germ-free and conventional Lobund-Wistar rats. *Journal of gerontology* **45**:B52-8.
1012 doi:10.1093/geronj/45.2.b52

1013 Song W, Veenstra JA, Perrimon N. 2014. Control of Lipid Metabolism by Tachykinin in Drosophila.
1014 *Cell Reports*. doi:10.1016/j.celrep.2014.08.060

1015 Staubach F, Baines JF, Kuenzel S, Bik EM, Petrov DA. 2012. Host species and environmental effects
1016 on bacterial communities associated with Drosophila in the laboratory and in the natural
1017 environment. *arXiv*. doi:10.48550/arxiv.1211.3367

1018 Storelli G, Defaye A, Erkosar B, Hols P, Royet J, Leulier F. 2011. Lactobacillus plantarum promotes
1019 Drosophila systemic growth by modulating hormonal signals through TOR-dependent nutrient
1020 sensing. *Cell metabolism* **14**:403–14. doi:10.1016/j.cmet.2011.07.012

1021 Tazume S, Umehara K, Matsuzawa H, Aikawa H, Hashimoto K, Sasaki S. 1991. Effects of germfree
1022 status and food restriction on longevity and growth of mice. *Jikken dobutsu Experimental animals*
1023 **40**:517–22.

1024 Team RC. 2024. R: A language and environment for statistical computing.

1025 Toprak U, Hegedus D, Doğan C, Güney G. 2020. A journey into the world of insect lipid metabolism.
1026 *Arch Insect Biochem Physiol* **104**:e21682. doi:10.1002/arch.21682

1027 Turnbaugh PJ, Ley RE, Mahowald MA, Magrini V, Mardis ER, Gordon JI. 2006. An obesity-associated
1028 gut microbiome with increased capacity for energy harvest. *Nature* **444**:1027.
1029 doi:10.1038/nature05414

1030 Valenzano D, Benayoun BA, Singh P, Zhang E, Etter PD, Hu C-K, Clément-Ziza M, Willemsen D, Cui
1031 R, Harel I, Machado BE, Yee M-C, Sharp SC, Bustamante CD, Beyer A, Johnson EA, Brunet A.
1032 2015. The African Turquoise Killifish Genome Provides Insights into Evolution and Genetic
1033 Architecture of Lifespan. *Cell* **163**:1539–1554. doi:10.1016/j.cell.2015.11.008

1034 Vijay-Kumar M, Aitken JD, Carvalho FA, Cullender TC, Mwangi S, Srinivasan S, Sitaraman SV,
1035 Knight R, Ley RE, Gewirtz AT. 2010. Metabolic Syndrome and Altered Gut Microbiota in Mice
1036 Lacking Toll-Like Receptor 5. *Science* **328**:228–231. doi:10.1126/science.1179721

1037 Wang Y, Staubach F. 2018. Individual variation of natural D.melanogaster-associated bacterial
1038 communities. *FEMS Microbiol Lett* **365**:fny017. doi:10.1093/femsle/fny017

1039 Watnick PI, Jugder B-E. 2020. Microbial Control of Intestinal Homeostasis via Enteroendocrine Cell
1040 Innate Immune Signaling. *Trends Microbiol* **28**:141–149. doi:10.1016/j.tim.2019.09.005

1041 Wilkinson JE, Burmeister L, Brooks SV, Chan C-C, Friedline S, Harrison DE, Hejtmancik JF, Nadon
1042 N, Strong R, Wood LK, Woodward MA, Miller RA. 2012. Rapamycin slows aging in mice:
1043 Rapamycin slows aging in mice. *Aging Cell* **11**:675–682. doi:10.1111/j.1474-9726.2012.00832.x

1044 Williams GC. 1957. Pleiotropy, natural selection, and the evolution of senescence. . *Evolution* **11**.

1045 Wong A, Dobson AJ, Douglas AE. 2014. Gut microbiota dictates the metabolic response of
1046 Drosophila to diet. *The Journal of Experimental Biology* **217**:1894–1901. doi:10.1242/jeb.101725

1047 Wong AC-N, Chaston JM, Douglas AE. 2013. The inconstant gut microbiota of Drosophila species
1048 revealed by 16S rRNA gene analysis. *ISME J* **7**:1922–1932. doi:10.1038/ismej.2013.86

1049 Wong AC-N, Dobson AJ, Douglas AE. 2014. Gut microbiota dictates the metabolic response of
1050 Drosophila to diet. *J Exp Biology* **217**:1894–1901. doi:10.1242/jeb.101725

1051 Zane F, Bouzid H, Marmol SS, Brazane M, Besse S, Molina JL, Cansell C, Aprahamian F, Durand S,
1052 Ayache J, Antoniewski C, Todd N, Carré C, Rera M. 2023. Smurfness-based two-phase model of
1053 ageing helps deconvolve the ageing transcriptional signature. *Aging Cell* **22**:e13946.
1054 doi:10.1111/acel.13946

1055 Zhang A, Meecham-Garcia G, Hong CN, Xie P, Kern CC, Zhang B, Chapman H, Gems D. 2024.
1056 Characterization of Effects of mTOR Inhibitors on Aging in Caenorhabditis elegans. *J Gerontol,*
1057 *Ser A: Biol Sci Méd Sci* **79**:glae196. doi:10.1093/gerona/glae196

1058

1059

1060 ## Supplementary figure legends

1061

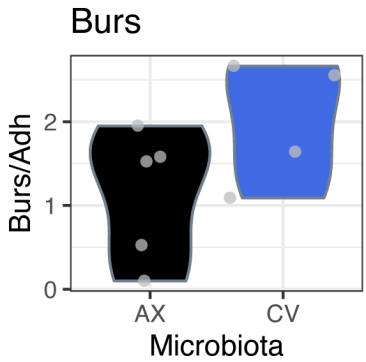

1062

1063 **Figure S1. Microbiota do not alter intestinal *Burs* expression.** Expression was quantified by RT-
1064 qPCR (using cDNA generated from midgut to complement RNA-seq data) because transcripts were
1065 not quantified from RNA-seq data (Figure 1). No significant difference in expression was detected (t=-
1066 1.65, p=0.15). AX=axenic, CV=conventionally-reared. Expression was quantified relative to *Adh*, as a
1067 housekeeping gene that RNAseq data showed to not be influenced by microbiota (Figure S2)

1068

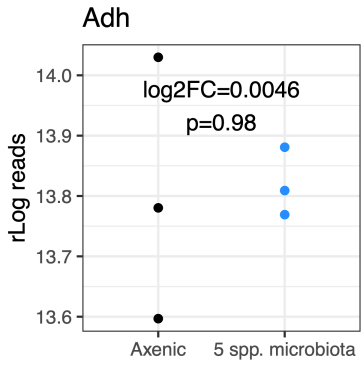

1069

1070 **Figure S2. Microbiota do not alter intestinal *Adh* expression.** Expression was quantified from public
1071 RNAseq data (Bost et al., 2018). Statistics show log2 fold-change and p-value (unadjusted) from
1072 DESeq2 analysis of reads quantified with Salmon.

1073

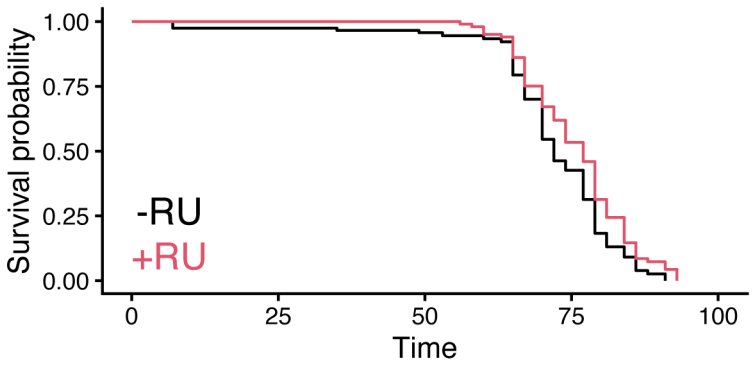

1074

1075 **Figure S3. Lifespan extension in conventional flies by induction of an independent *Tk*^{RNAi}.** To
1076 validate result show in Figure 2A a distinct construct (Vienna *Drosophila* Stock Center #25800) was

1077 expressed under control of *DaGS.* Log-rank test p<0.01. -RU condition 108 deaths, 43 censors; +RU
1078 condition 124 deaths, 26 censors.
1079

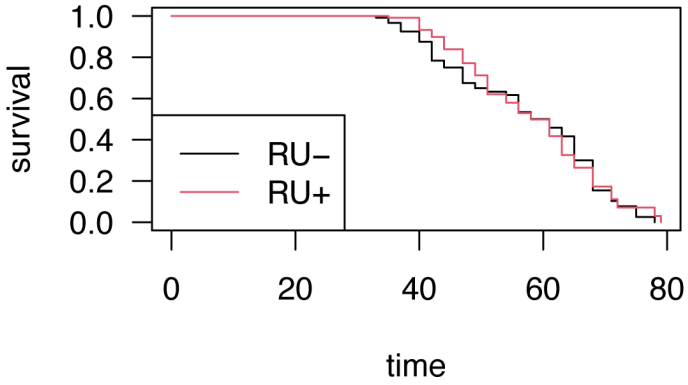

1080
1081 **Figure S4. Lifespan extension by feeding RU to CR *DaGS;UAS-Tk^{RNAi}* flies is not attributable to**
1082 **off-target effects of RU or GeneSwitch activation.** Kaplan-Meier plot shows impact of feeding RU to
1083 *DaGS/+* flies reared with complete microbiota. No effect of RU was detected (Cox Proportional Hazards
1084 p=0.5).
1085

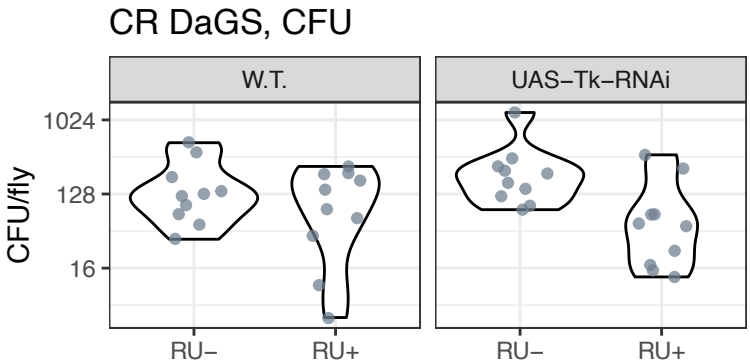

1086
1087 **S5 CFU. *TkRNAi* does not affect bacterial load in CR flies.** Violin plots show CFUs of conventionally-
1088 reared female adults of the indicated genotypes (all with *DaGS*) , after one week of feeding on RU or
1089 vehicle control. All conditions n=10. No effects were detected of presence/absence of *UAS-Tk-RNAi*
1090 (ANOVA of log CFU counts, p=0.32), RU (p=0.23), nor genotype:RU interaction (p=0.25).

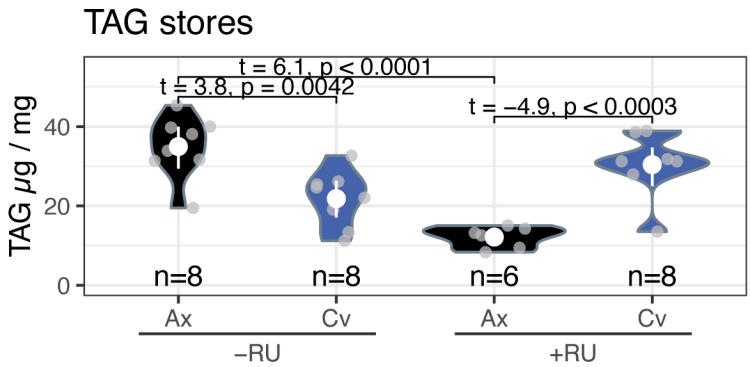

1091

1092 **Figure S6. Interactive effect of *TkRNAi* and microbiota on TAG levels confirmed with**
1093 **independent RNAi construct.** The experiment presented in Figure 2E (which used construct
1094 V330743) was repeated with an independent construct (V103668). The same result was replicated.
1095 Violin plots show density of datapoints, mean±CI95 given in white. ANOVA (Type 3 tests),
1096 microbiota:RU $F_{1,26}$=37.86, p=1.66e-06. Statistics on brackets are from *post-hoc* EMM analyses of
1097 linear model, when significant differences were detected.
1098

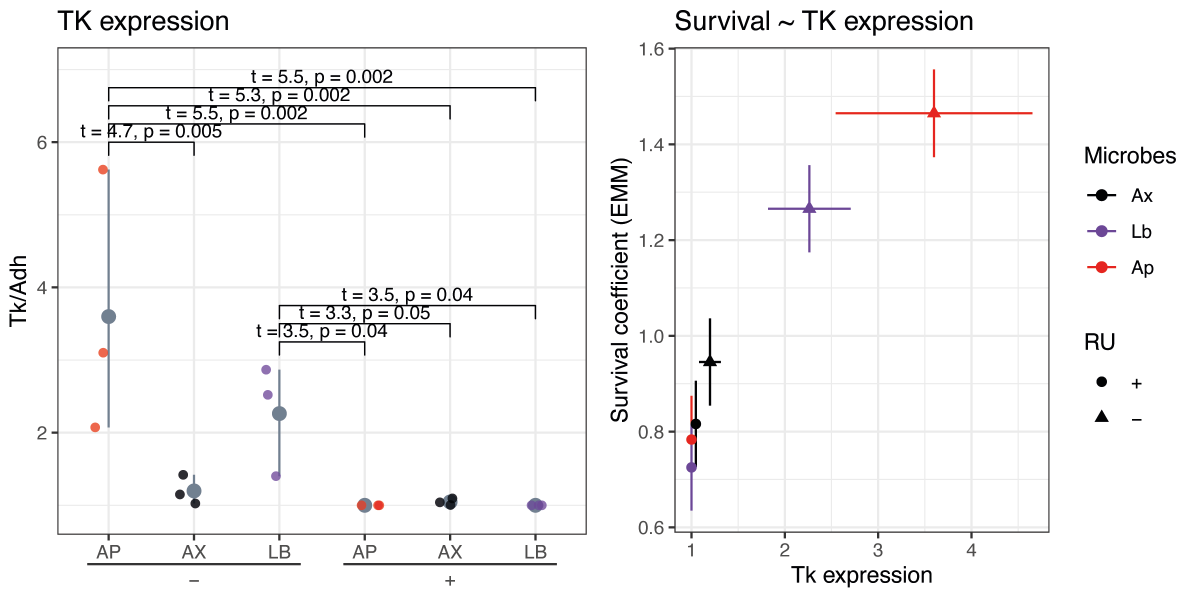

1099
1100 **Figure S7. Modulation of *Tk* expression by microbiota correlates lifespan outcome. A.** RT-qPCR
1101 indicates elevated *Tk* expression in *Ap*-flies above levels in axenics and *Lb*-flies, and above levels in
1102 all conditions expressing Tk^{RNAi}. Expression in *Lb*-flies was significantly greater than in conditions
1103 expressing Tk^{RNAi}, but not significantly greater than axenics without Tk^{RNAi} expression. Statistics on
1104 brackets are from *post-hoc* EMM analyses of linear model, when significant differences were detected.
1105 **B.** *Tk* expression differences across microbiota and Tk^{RNAi} conditions correlate lifespan differences. *Tk*
1106 expression from panel A is plotting against survival coefficients of lifespan experiment shown in Figure
1107 3c-d.
1108

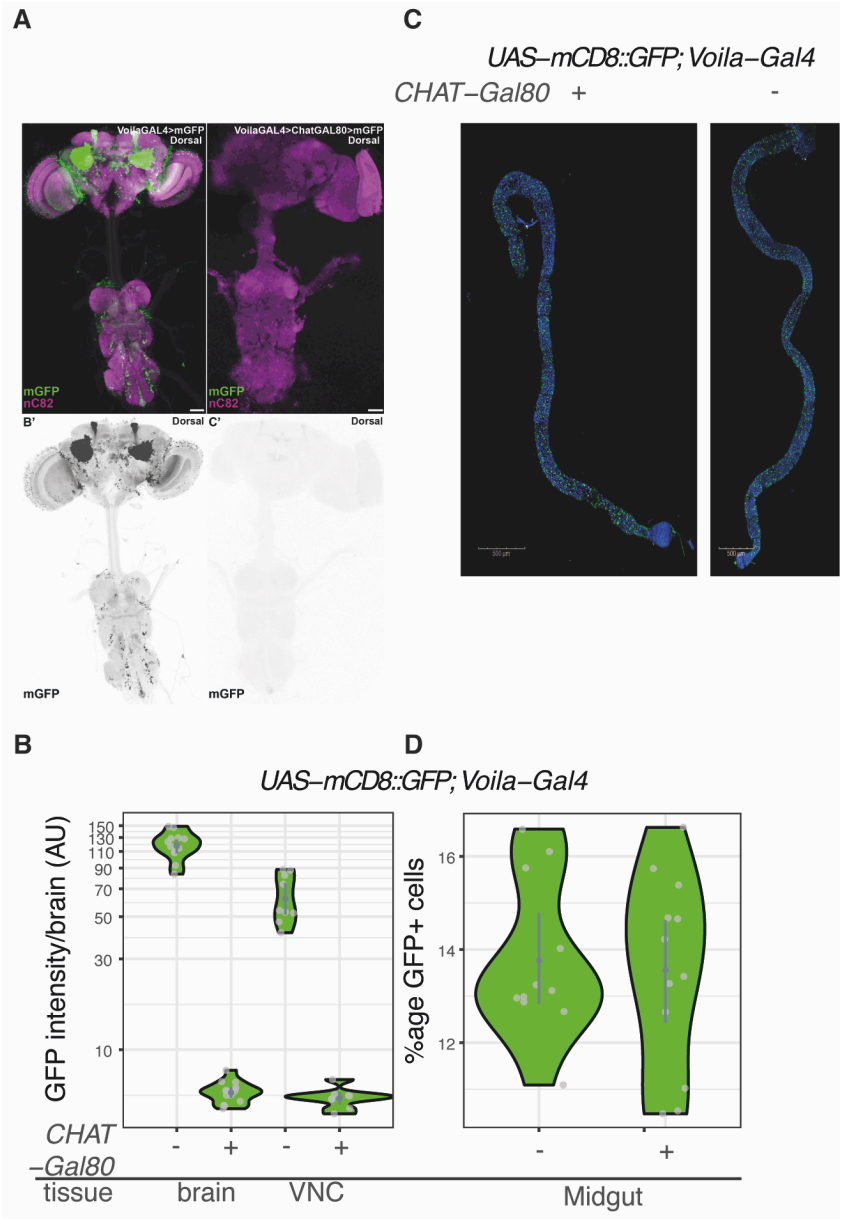

Figure S8. Intersectional Gal80 strategy to direct Gal4 activity to enteroendocrine cells, sparing CNS. As per Medina et al (Medina et al., 2024), we tested the capacity of Gal80 expressed under control of the *ChAT* promoter to repress Gal4 expressed under control of the *Voila* promoter, assayed by expression of *UAS-mCD8::GFP.* **A.** Representative confocal micrographs of CNS, and **B.** Quantification of Voila>GFP intensity in brain and CNS, in presence/absence of *Voila Gal80*. **C.** Representative confocal micrographs of midgut (region 4). **D.** Number of GFP+ cells/ROI in presence/absence of *Voila Gal80.*

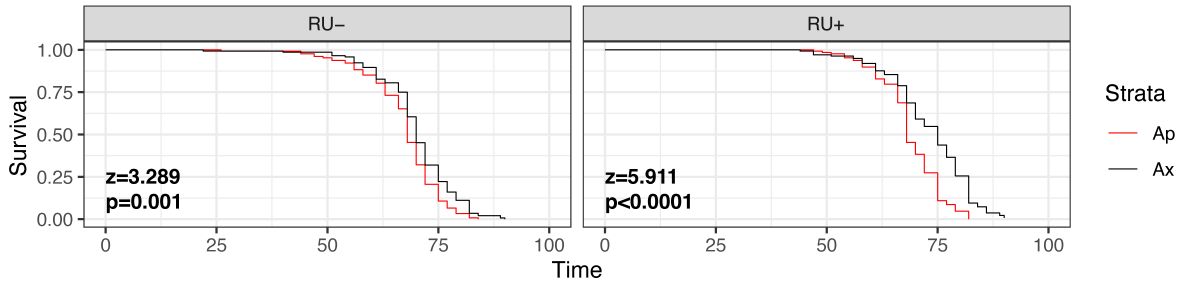

1118

1119 **Figure S9. *TkR99D*^{RNAi} induction in enterocytes does not block impact of *A. pomorum* on**
1120 **lifespan.** Expression was driven with *Mex1-GeneSwitch*. Statistics in panel from Cox proportional
1121 hazards model, reporting post-hoc (EMM) analysis for effect of RU per microbiota condition.

1122

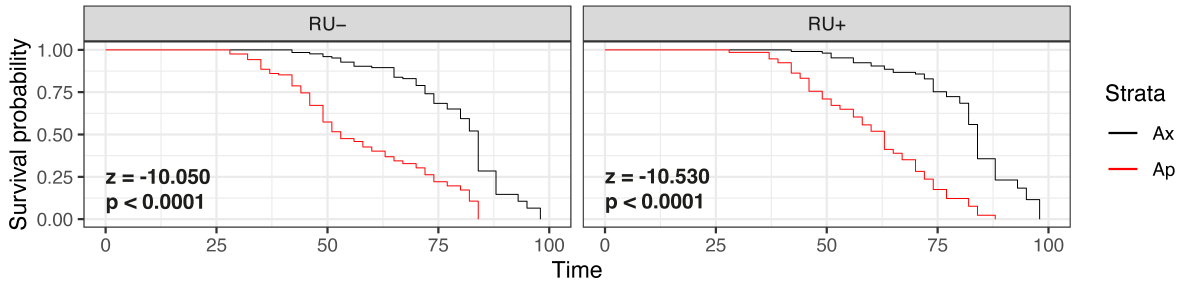

1123

1124 **Figure S10. *AkhR*^{RNAi} induction in fat body (and gut) does not block impact of *A. pomorum* on**
1125 **lifespan.** Expression was driven with *S106-GeneSwitch*. Statistics in panel from Cox proportional
1126 hazards model, reporting post-hoc (EMM) analysis for effect of RU per microbiota condition.

1127